Swiss Journal of Palaeontology

RESEARCH ARTICLE Open Access

A Pliocene–Pleistocene continental biota from Venezuela

Jorge D. Carrillo-Briceño[1*], Rodolfo Sánchez[2], Torsten M. Scheyer[1], Juan D. Carrillo[3,4], Massimo Delfino[5,6], Georgios L. Georgalis[1], Leonardo Kerber[7,8], Damián Ruiz-Ramoni[9], José L. O. Birindelli[10], Edwin-Alberto Cadena[11,15], Aldo F. Rincón[12], Martin Chavez-Hoffmeister[13], Alfredo A. Carlini[14], Mónica R. Carvalho[15], Raúl Trejos-Tamayo[16,17], Felipe Vallejo[16,17], Carlos Jaramillo[15,17,18], Douglas S. Jones[19] and Marcelo R. Sánchez-Villagra[1*]

Abstract

The Pliocene–Pleistocene transition in the Neotropics is poorly understood despite the major climatic changes that occurred at the onset of the Quaternary. The San Gregorio Formation, the younger unit of the Urumaco Sequence, preserves a fauna that documents this critical transition. We report stingrays, freshwater bony fishes, amphibians, crocodiles, lizards, snakes, aquatic and terrestrial turtles, and mammals. A total of 49 taxa are reported from the Vergel Member (late Pliocene) and nine taxa from the Cocuiza Member (Early Pleistocene), with 28 and 18 taxa reported for the first time in the Urumaco sequence and Venezuela, respectively. Our findings include the first fossil record of the freshwater fishes *Megaleporinus*, *Schizodon*, *Amblydoras*, *Scorpiodoras*, and the pipesnake *Anilius scytale*, all from Pliocene strata. The late Pliocene and Early Pleistocene ages proposed here for the Vergel and Cocuiza members, respectively, are supported by their stratigraphic position, palynology, nannoplankton, and $^{86}Sr/^{88}Sr$ dating. Mammals from the Vergel Member are associated with the first major pulse of the Great American Biotic Interchange. In contrast to the dry conditions prevailing today, the San Gregorio Formation documents mixed open grassland/forest areas surrounding permanent freshwater systems, following the isolation of the northern South American basin from western Amazonia. These findings support the hypothesis that range contraction of many taxa to their current distribution in northern South America occurred rapidly during at least the last 1.5 million years.

Keywords: Neogene, Neotropics, Northern South America, Urumaco sequence, Paleodiversity, *Megaleporinus*, *Amblydoras*, *Anilius*, Camelidae, *Chapalmalania*

Introduction

During the Miocene, the coastal marine areas of northern South America arid regions of northern Colombia and northwestern Venezuela today were influenced by a complex hydrographic system that flowed mostly from western Amazonia into the Proto-Caribbean Sea (Díaz de Gamero 1996; Hoorn et al. 2010; Aguilera et al. 2013).

Some of the best-known terrestrial and aquatic vertebrate faunas that document the changing biodiversity during that time are preserved in the middle–late Miocene Socorro and Urumaco formations, in northwestern Venezuela (e.g., Sánchez-Villagra et al. 2010). Diverse assemblages of aquatic and terrestrial vertebrates, such as fishes, amphibians, turtles, crocodylians, snakes, and mammals, have been reported from these sedimentary units that accumulated in a coastal plain-delta system (Lundberg and Aguilera 2003; Aguilera 2004; Linares 2004; Aguilera et al. 2006; Hsiou and Albino 2010; Lundberg et al. 2010; Quiroz and Jaramillo 2010; Sánchez-Villagra et al. 2010; Aguilera et al. 2013; Scheyer et al. 2013,

Editorial handling: Daniel Marty

*Correspondence: jorge.carrillo@pim.uzh.ch; m.sanchez@pim.uzh.ch
[1] Universität Zürich, Paläontologisches Institut und Museum, Karl-Schmid-Straße 4, 8006 Zurich, Switzerland
Full list of author information is available at the end of the article

2019; Forasiepi et al. 2014; Rincón et al. 2015; Scheyer and Delfino 2016; Aguirre-Fernández et al. 2017a, b; Carrillo-Briceño et al. 2018b; Delfino and Sánchez-Villagra 2018; Cadena et al. 2020; and references therein).

The hydrographic connections between western Amazonia and the Proto-Caribbean Sea were home for many freshwater species, with a continuum of the biota from the Amazonian forest into northwestern Venezuela during the Miocene (Jaramillo et al. 2010). By the late Miocene to early Pliocene, extreme environmental changes took place in the region (Jaramillo et al. 2010; Sánchez-Villagra et al. 2010; Scheyer et al. 2013). These changes were linked to major hydrographic processes that occurred as a consequence of the northern Andes uplift (Mora et al. 2010; Albert et al. 2018), which may have led to the separation between the northern peripheral drainages of western Amazonia, creating habitat partitioning that drove vicariance in many groups including fishes, crocodylians, turtles, and aquatic snake communities (Lundberg et al. 1998, 2010; Schargel et al. 2007; Sánchez-Villagra et al. 2010; Scheyer et al. 2013; Cadena et al. 2020). The transition between the Urumaco Formation and the overlying latest Miocene–early Pliocene Codore Formation (Quiroz and Jaramillo 2010) documents a major turn in the dynamics of the sedimentary and environmental conditions of the region. The continental facies of the Codore Formation (El Jebe and Algodones members) were deposited in floodplain environments (exposed during long periods to subaerial conditions) (Quiroz and Jaramillo 2010).

Although the environmental and faunal changes that occurred during the Miocene–Pliocene transition in the Urumaco region and adjacent areas are unmistakable (e.g., Jaramillo et al. 2010; Lundberg et al. 2010; Scheyer et al. 2013), the record of Pliocene–Pleistocene terrestrial and freshwater vertebrates in the Urumaco sequence still consists of isolated reports, such as from the Codore and San Gregorio formations, that resulted from occasional prospecting in the area. Some terrestrial vertebrates have been described from the continental facies of the Codore Formation (El Jebe and Algodones members), including a Jabiru stork (Walsh and Sánchez 2008), sloths (Carlini et al. 2006a, b), glyptodontids (Carlini et al. 2008a, b), and meridiungulates (Carrillo et al. 2018). A skull and an isolated ear bone of iniid dolphins (Aguirre-Fernández et al. 2017a, b) were recovered from the Chiguaje Member of the Codore Formation, representing a transgressive event associated with a low-energy coastal lagoon or bay (Quiroz and Jaramillo 2010; Carrillo-Briceño et al. 2015).

The Vergel Member is the lowest member of the San Gregorio Formation and overlies the Algodones Member of the Codore Formation (Quiroz and Jaramillo 2010). The fossil record of this Member includes thorny catfish (Aguilera et al. 2013), crocodylians (Scheyer et al. 2013), terrestrial sloths, glyptodontids, pampatheriids and dasypodid armadillos (Carlini et al. 2008c, 2018; Carlini and Zurita 2010; Vucetich et al. 2010; Zurita et al. 2011; Castro et al. 2014), notoungulates (Carrillo et al. 2018), a procyonid (Forasiepi et al. 2014), and caviomorph rodents (Vucetich et al. 2010).

Based on thorny catfish remains from the Vergel Member as well as other freshwater Siluriformes from the Pliocene of the Cocinetas Basin in the Guajira Peninsula (northern Colombia), Aguilera et al. (2013) suggested the existence of a probable "last hydrographic connection" between northern South American and western Amazonian basins between 3.2 and 1.7 Ma. Diverse reports (e.g., Carlini and Zurita 2010; Vucetich et al. 2010; Aguilera et al. 2013; Scheyer et al. 2013; Castro et al. 2014; Forasiepi et al. 2014; Carlini et al. 2018; Carrillo et al. 2018) demonstrated the potential of the San Gregorio Formation to preserve evidence of the biota at the otherwise poorly sampled Pliocene–Pleistocene strata in this region of South America. Thus, our ongoing efforts continued throughout the 2007–2020 period in the search for microvertebrates and other fossils we report in this work.

Here, we present new terrestrial and aquatic vertebrates from the late Pliocene–Pleistocene San Gregorio Formation. Two different assemblages are described from the Vergel (lower) and Cocuiza (middle) members. A new paleoenvironmental interpretation, as well as new dating for the San Gregorio Formation, is proposed. Based on the taxonomic affinities of this fauna with those from the Orinoco/Amazonian systems, and Caribbean basins of Colombia and Venezuela, we discuss its paleogeographic and biochronologic significance. Our results shed light on the evolutionary history of the terrestrial and freshwater vertebrate faunas of the region, particularly during the transitional stage that preceded the major climatic shift of the Quaternary.

Geological and stratigraphical settings

The San Gregorio Formation is the youngest unit of the Urumaco stratigraphic section (see Quiroz and Jaramillo 2010). This unit overlies unconformably the Algodones Member of the Codore Formation (Fig. 1B) and crops out northwest of the town of Urumaco, Falcón State, in northwestern Venezuela (Fig. 1A). The San Gregorio Formation is 570 m thick at its type section (see Stainforth 1962; Rey 1990; Hambalek et al. 1994), which is located 2 km east of the village of San Gregorio and one km east of the Ulé-Amuay pipeline. The age of the San Gregorio Formation has been considered either Pliocene or Early Pleistocene based on its stratigraphic position and palynological data (e.g., Rey 1990;

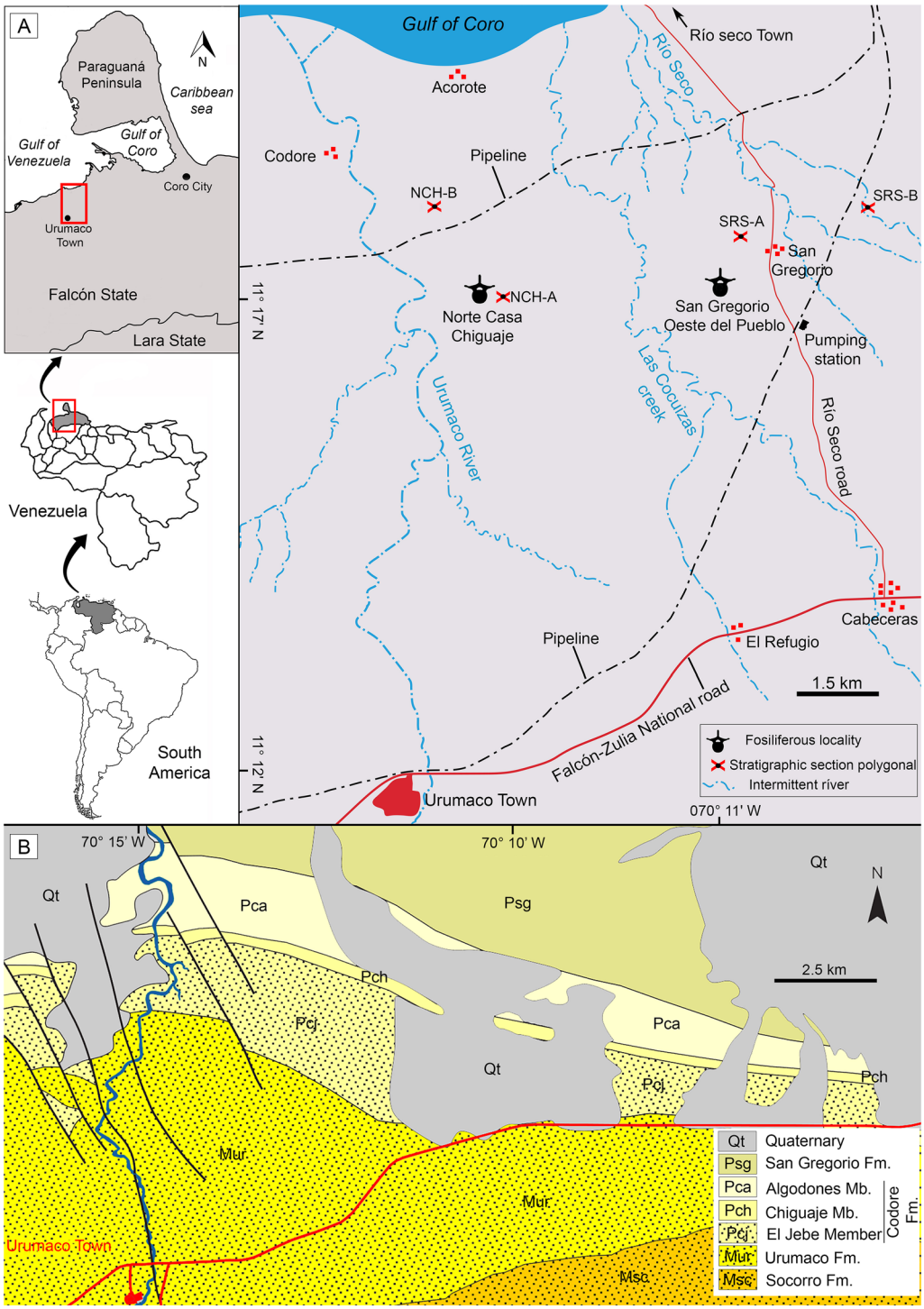

Fig. 1 Geographical and geological location. **A** Location map of the fossiliferous localities of the San Gregorio Formation. Stratigraphic section polygonal: Northward Chiguaje Hill "NCH" (see Additional file 1) and San Gregorio Río Seco "SGRS" (see Additional file 2). **B** Generalized geological map near the town of Urumaco showing the outcropping geological units in the area (modified after Quiroz and Jaramillo 2010). *Fm.* Formation, *Mb.* Member

Hambalek et al. 1994). Recently, an age of approximately 1.8 Ma was suggested for the boundary between the top of the Algodones Member and the base of the San Gregorio Formation and supported by multiple foraminiferal, nannoplankton, and magnetic stratigraphic studies (Carrillo et al. 2018, table 12, fig. 28).

Stainforth (1962) suggested the division of the San Gregorio Formation into three formal members: Vergel (lower), Cocuiza (middle), and Río Seco (upper). The Vergel Member is a ~ 260 m thick sequence (Hambalek et al. 1994) composed of interbedding mudstones, sandstones, and sparse conglomeratic beds (Stainforth 1962) that denote fluvial environments (e.g., braided rivers) and alluvial fans (Rey 1990; Hambalek et al. 1994; Quiroz and Jaramillo 2010). Overlying conformably the Vergel Member is the Cocuiza Member, an 80-m thick sequence (in its type section), dominated by marine deposits with low to moderate energy coastline, and local presence of terrigenous sediments (Rey 1990; Hambalek et al. 1994; Mihaljević et al. 2010). The Río Seco Member (142 m thick in its type section) overlies the Cocuiza Member and is characterized by interbedding of mudstones, sandstones, and conglomerates representing a sedimentary accumulation in fluvial environments and alluvial fans (Rey 1990).

The fossiliferous content of the "Norte Casa Chiguaje" locality (NCC) in the Vergel Member (Figs. 1A, 2A–F and 3A, B) and the "San Gregorio Oeste del Pueblo" locality (SGOP) in the Cocuiza Member (Figs. 1A, 2G, H and 3C) are described. Both localities crop out in badlands, offering excellent exposures that allowed the identification of fossil-bearing layers in the field. The NCC locality and its section "S1" (Fig. 3B) is part of the "Section Northward Chiguaje Hill" (NCH) (Figs. 1A and 3A), which is presented in more detail in Additional file 1. The "S1" section is characterized by unconsolidated yellowish-orange to light-brown fine sandstones with a thin (~ 30 cm) consolidated conglomeratic layer of a light–dark gray matrix with well-rounded to sub-rounded clasts of up to 25 mm in diameter (Fig. 2A–C). This conglomeratic layer is well exposed along 180 m with a direction of N 55° W (Fig. 2A, B). Some cranial and postcranial elements were collected from the sandstones underlying/overlying the conglomerate layer. Most of the fossils collected in the conglomeratic layer were small/micro elements, and in many cases were fractured and incomplete, suggesting a taphonomic effect of transport. The mammalian remains described in Carlini et al. (2008c, 2018), Vucetich et al. (2010), Zurita et al. (2011), Castro et al. (2014), Forasiepi et al. (2014), and Carrillo et al. (2018) were collected in this locality. A late Pliocene age has been estimated for the Vergel Member based on its stratigraphic position and mammalian association (Carlini and Zurita 2010; Zurita et al. 2011; Castro et al. 2014).

The SGOP locality section "S2" (Figs. 1A and 3C) is a fossiliferous locality discovered in 2019. A detailed stratigraphic section for locality "S2" is presented (Fig. 3C); however, we have not been able to correlate it to either the NCH (Figs. 1A and 3A; Additional file 1) or the San Gregorio Río Seco (SGRS) (Fig. 1; Additional file 2) sections. Field observations and its marine fossil content suggest that the SGOP locality might belong to the middle section of the Cocuiza Member. The SGOP locality is characterized by an interbedding of clay-rich to coarse sandstones with abundant marine invertebrates, including sirenian remains, and some conglomeratic sandstones layers (Fig. 2G, H). The conglomerates are consolidated and dark-brown in color with well-rounded to sub-rounded clasts, bearing disarticulated terrestrial vertebrates (mammals and reptiles), suggesting intermittent flows of terrigenous sediments to the littoral environment. A Pliocene age was estimated for the Cocuiza Member based on palynomorphs (Stainforth 1962; Hambalek et al. 1994).

Materials and methods

The vertebrate fossils correspond to a total sample of 1746 cranial and postcranial elements of freshwater fishes, amphibians, reptiles, and mammals (Figs. 4, 5, 6, 7, 8, 9, 10, 11, 12, 13, 14, 15, 16, 17, 18, 19, 20, 21, 22, 23, 24, 25, 26, 27, 28, and 29, Table 1), recovered from the NCC (11° 17′ 52.9″ N, 070° 14′ 7.3″ W) and SGOP (11° 17′ 54.6″ N, 070° 11′ 24.6″ W) localities. The fossil specimens were collected by the authors (JDCB, RS, TMS, JDC, MD, EAC, AAC, and MRSV), and other collaborators during several field expeditions between 2007 and 2020. Large specimens were surface collected from the outcrops of both localities, while micro-vertebrates and microfossil remains (e.g., seeds and invertebrates) were found only in the NCC locality. A total of ~ 200 kg of conglomerates and sandstones were screen-washed using standard sieves with up to 0.5 mm mesh. The micro-specimens were sorted using a stereomicroscope. Images were captured with a Leica MZ16F multifocal stereomicroscope and a Scanning Electronic Microscope (JEOL JSM-6010). All the fossil specimens are housed in the paleontological collections of the Alcaldía Bolivariana de Urumaco, Falcón State, Venezuela, with the acronym AMU-CURS for vertebrates, and AMU-PB and AMU-PI for fossil plant and invertebrate remains, respectively.

Taxonomic identification involved an extensive bibliographic review and comparison with fossil and extant specimens housed at Argentina [Museo de La Plata (MLP); Museo Argentino de Ciencias Naturales Bernardino Rivadavia, Buenos Aires (MACN); Museo

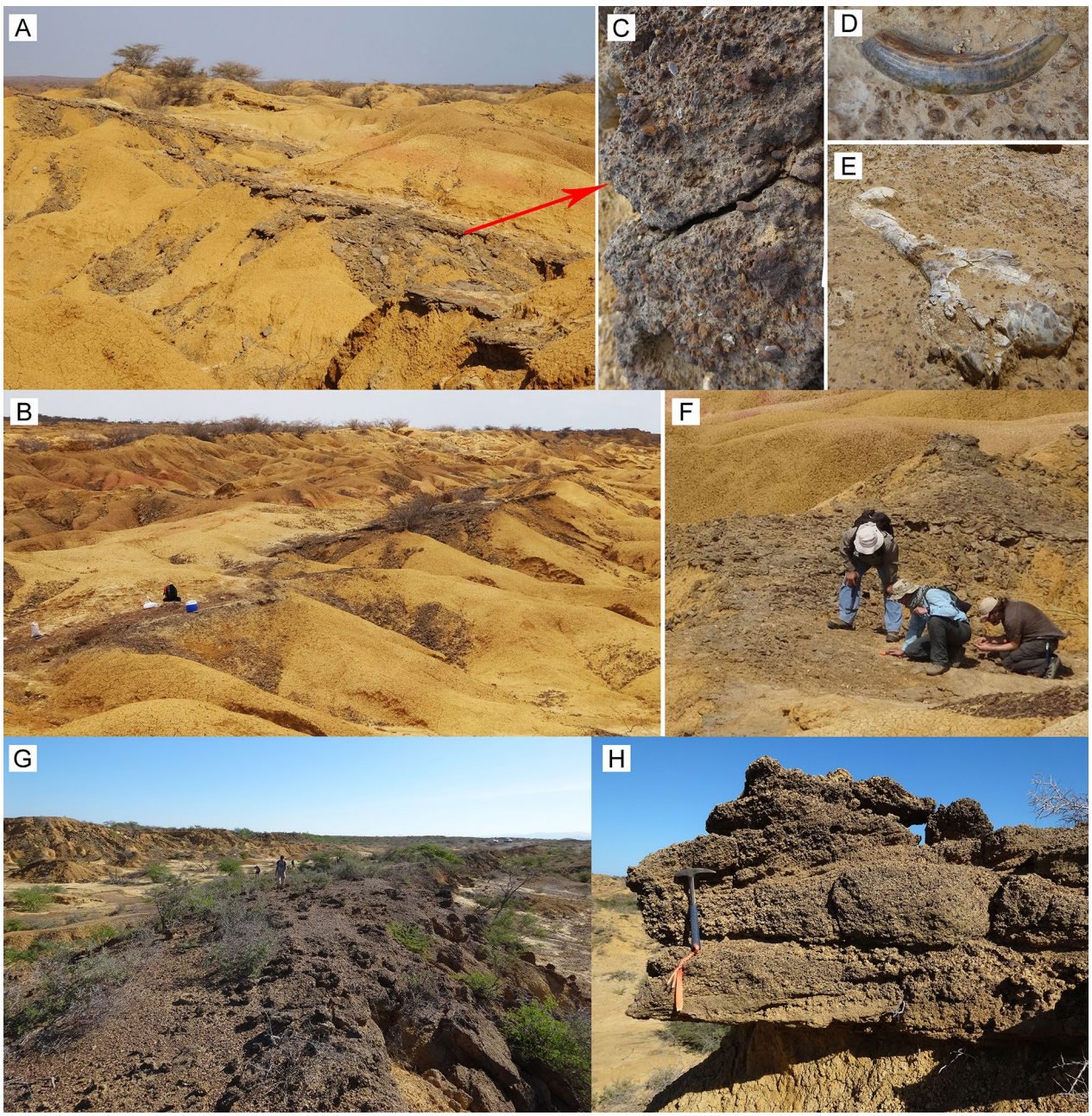

Fig. 2 Fossiliferous localities of the San Gregorio Formation outcrops. **A**–**F** Norte Casa Chiguaje locality. **C** Close-up of the conglomeratic-fossiliferous layer. **D**, **E** Tooth (**D**) and humerus (**E** AMU-CURS-62) of mammals in situ. **G**, **H** San Gregorio Oeste del Pueblo locality. **H** Example of the conglomeratic layers were disarticulated continental vertebrates remains were found. Pictures from authors JDCB (**A**–**D**, **G**, **H**) and EAC (**F**)

de Ciencias Naturales y Antropológicas J. C. Moyano, Mendoza (MCNAM-PV); Museo Paleontológico Egidio Feruglio, Trelew (MPEF PV); Laboratorio de Investigaciones en Evolución y Biodiversidad-Colección Paleontología de Vertebrados, Universidad Nacional de la Patagonia San Juan Bosco, Esquel, Chubut (LIEB-PV)], Austria [Naturhistorisches Museum, Vienna (NHMW)], Brazil [Museu Paraense Emilio Goeldi (MPEG-V); Paleontological collection of the Departamento Nacional de Produção Mineral, Rio de Janeiro (DNPM); Paleontological collection of the Universidade Federal do Acre (Campus Rio Branco), Rio

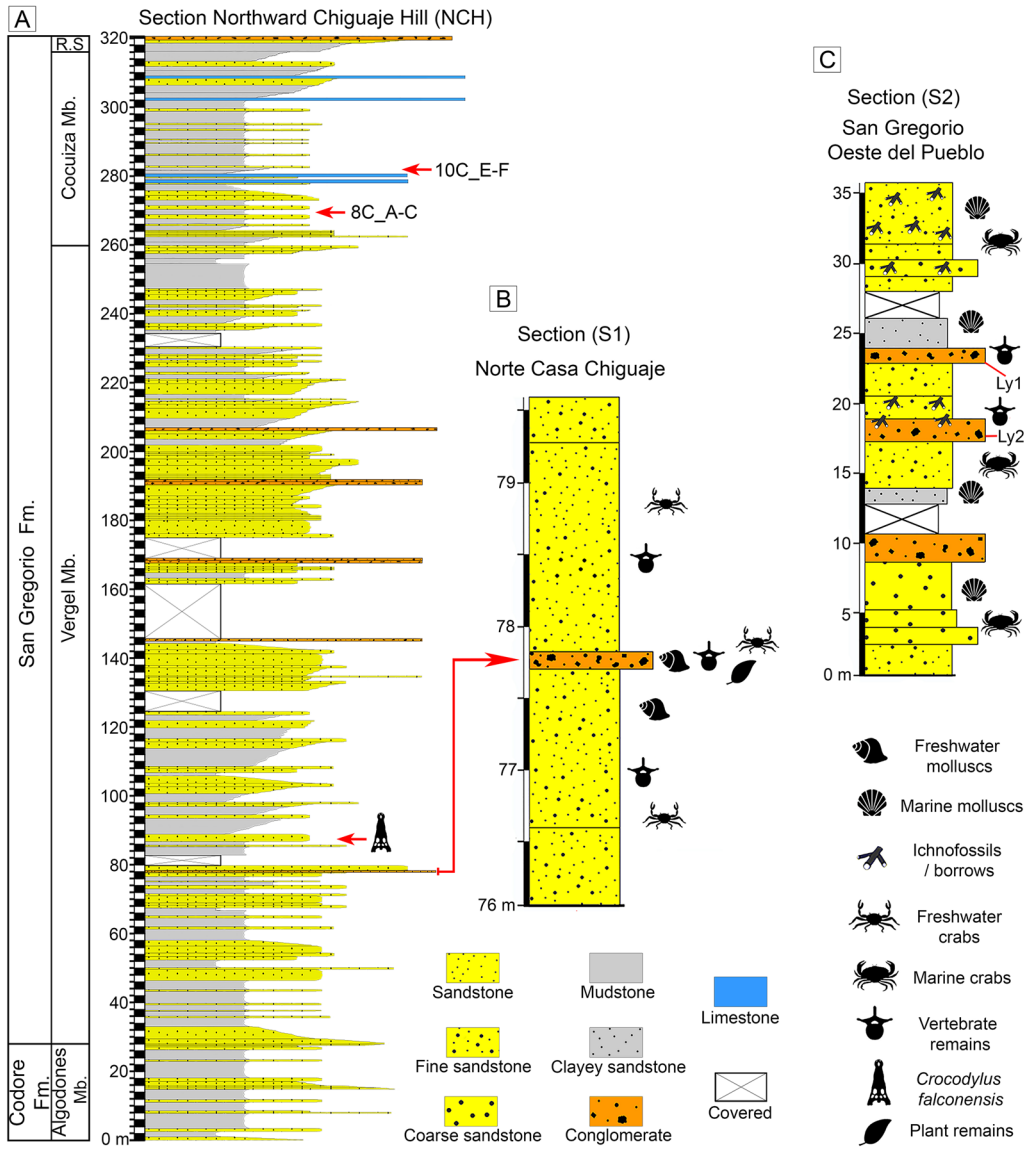

Fig. 3 Stratigraphic context of the San Gregorio Formation. **A** Generalized section of Northward Chiguaje Hill polygonal (NCH) (see Fig. 1); a section with more detail of the NCH is presented in Additional file 1. **B** Norte Casa Chiguaje locality section. **C** San Gregorio Oeste del Pueblo locality section. The "8C_A-C" and "10C_E-F" referred in the NCH section correspond molluscan shell samples used for $^{87}Sr/^{86}Sr$ analyses (see Additional file 5). *Fm.* Formation, *Mb.* Member, *R.S* Río Seco Member

Branco (UFAC)], Colombia [Instituto de Ciencias Naturales, Universidad Nacional de Colombia (ICN); Museo Geológico José Royo y Gómez, Servicio Geológico Colombiano, Bogotá (IGM); The Mapuka Museum of Universidad del Norte (MUNSTRI)], France [Muséum National d'Histoire Naturelle, Paris (MNHN)], Hungary [Hungarian Natural History Museum, Budapest (HNHM)], Italy [Massimo Delfino Herpetological Collection, Università di Torino (MDHC)], Poland [Institute of Systematics and Evolution of Animals of the Polish Academy of Sciences, Krakow (ZZSiD)], Spain [Museo Nacional de Ciencias Naturales, Madrid (MNCN)], Switzerland [Natural History Museum of Basel (NMB); Paleontological Institute and Museum at the University of Zurich (PIMUZ)], United Kingdom [Natural History Museum, London (NHMUK)], USA [Academy of Natural Sciences of Drexel University, Philadelphia (ANSP); American Museum of Natural History, New York (AMNH); California Academy of Sciences, San Francisco (CAS); Field Museum of

Natural History, Chicago (FMNH); Florida Museum of Natural History, Gainesville (FLMNH); Natural History Museum Los Angeles County (LAM), Vertebrate collection of the La Brea Tar Pits and Museum, Los Angeles, California], and Venezuela [Centro de Investigaciones Antropológicas, Arqueológicas y Paleontológicas of the Universidad Experimental Francisco de Miranda (CIAAP, UNEFM-PF); Colección de Paleontología del Instituto Venezolano de Investigaciones Científicas (IVIC); Museo de Ciencias de Caracas (MCNC); Museo de Biología de la Universidad del Zulia (MBLUZ); Museo de la Estación Biológica Rancho Grande (EBRG); Museo de Historia Natural La Salle (MHNLS), Fundación La Salle de Ciencias Naturales, Caracas].

In order to estimate the generic richness and assess the completeness of the sampling, we performed a rarefaction and extrapolation sampling curve (Colwell et al. 2012). Rarefaction curves were made for the two best sampled clades (mammals and fishes) recorded in the NCC locality. We estimated generic richness because most of the specimens could not be identified to species level. We included specimens identified to genus level, and if a specimen was only identified to a more inclusive clade, we treated it as a different genus. For example, as Mylodontidae is not represented by any genus, a specimen was referred as a mylodontid undetermined genus (Table 1). We computed and plotted the rarefaction and extrapolation sampling curves using the iNEXT package (Hsieh et al. 2016) available in R (R core team 2019).

Dating of the San Gregorio Formation

We analyzed 30 palynological samples (Additional file 3) from two stratigraphic columns spanning the entire San Gregorio Formation, including the NCH (Figs. 1A and 3A; Additional file 1) and SGRS (Fig. 1; Additional file 2) sections, plus 29 samples from the Cocuiza Member for micropaleontology (nannoplankton and foraminifera) (Additional file 4). Five marine low-Mg calcitic shell molluscan fossils (pectinids) from the NCH section and four from the Rio Seco Oil Pipeline section (Cocuiza Member) were prepared for $^{87}Sr/^{86}Sr$ geochronological analyses (Additional file 5).

The palynological samples were prepared following standard techniques at Instituto de Investigaciones en Estratigrafía (IIES), Universidad de Caldas, Colombia (Traverse 2007). The procedure included the processing of 15 g of rock in hydrochloric acid (HCl) for 12 h to remove calcareous material. Hydrofluoric acid (HF) was then added to remove silicates. The organic residue was cleaned using ultrasonic equipment, and then concentrated by centrifugation, followed by mounting of a first cover slide in a solution of polyvinyl alcohol. A second cover slide was mounted following the same protocol described above after oxidation of the residue with nitric acid (HNO3). Canadian balsam was used to seal both mounted slides.

A total of 29 samples were prepared for stratigraphic purposes using the standard technique of smear slides (Backman and Shackleton 1983). Microscopic examinations of calcareous nannofossils were performed in a Nikon light microscope at 1000× magnification. We apply the standard biozonation of Martini (1971) for tropical areas and use the biochronology proposed by Backman et al. (2012).

Twenty-two rock samples were prepared for foraminifera (Thomas and Murney 1985). Samples were treated with hydrogen peroxide (H_2O_2) [5%] to eliminate the organic matter. Each sample was washed trough a 63-µm sieve to remove the finest sediment. The residue was dried at 50 °C in an oven for 24 h, and separated into the following fractions: > 63 µm, > 125 µm, > 250 µm, and > 425 µm. Fractions were analyzed using a stereomicroscope Nikon SMZ 1500. Most of the foraminifera extracted from the sediment were benthic, and our taxonomic classification followed van Morkhoven et al. (1986), Bolli et al. (1994), Kaminski and Gradstein (2005), and Holbourn et al. (2013).

Powdered calcite samples were drilled from the interior of each specimen using a hand-held Dremel tool with a carbide dental burs. Approximately 0.01 to 0.03 g of powder was recovered from each fossil sample, and these were analyzed according to standard techniques (Kirby et al. 2008). The powdered samples were dissolved in 100 µL of 3.5 N HNO_3 and then loaded onto cation exchange columns packed with strontium-selective crown ether resin (Eichrom Technologies, Inc.) to separate Sr from other ions. Sr isotope analyses were performed on a Micromass Sector 54 Thermal Ionization Mass Spectrometer equipped with seven Faraday collectors and one Daly detector in the Department of Geological Sciences at the University of Florida. Sr was loaded onto oxidized tungsten single filaments and run in triple collector dynamic mode. Data were acquired at a beam intensity of about 1.5 V for 88Sr, with corrections for instrumental discrimination made assuming $^{86}Sr/^{88}Sr = 0.1194$. Errors in measured $^{87}Sr/^{86}Sr$ are better than ± 0.00002 (2σ), based on long-term reproducibility of NIST 987 ($^{87}Sr/^{86}Sr - 0.71024$). Age estimates were determined using the appropriate portion of Look-Up Table Version 4:08/03 associated with the Sr isotopic age model of McArthur et al. (2001).

Results

Dating of the San Gregorio Formation

Vergel Member: Most of the pollen samples were sterile (22 out of 30, Additional file 3). The pollen record of meters 237–262 of NCH section, which corresponds to the top 40 m of the Vergel Member (Additional file 1), includes the last occurrence datum (LAD) of *Bombacacidites nacimientoensis*, *Retitrescolpites*? *irregularis*, and *Rhoipites guianensis*.

Cocuiza Member: Strontium ratios ranged between 0.709100 and 0.709342 (Additional file 5). Five of the samples yielded ratios higher than, or indicative of, modern seawater suggesting diagenetic alteration. Two others yielded latest Pleistocene ages, but were statistically inseparable from modern seawater. Two samples that seemed pristine and did not show evidences of probable alteration yielded Early Pleistocene ages when compared to the global seawater $^{87}Sr/^{86}Sr$ curve for the Neogene (McArthur et al. 2001). The first, from NCH section, yielded a mean age of 1.38 ± 0.06 Ma. The other, SGRS section, yielded a mean age of 1.59 ± 0.05 Ma (Additional file 5) (Fig. 30).

Calcareous nannoplankton results show poor to moderate preservation and abundant Paleogene and Neogene reworked microfossils. The youngest identified assemblage is composed of *Calcidiscus macintyrei*, *Helicosphaera sellii*, *Gephyrocapsa* spp., and *Pseudoemiliania lacunosa*. Of the twenty-two samples analyzed for foraminifera, eight were barren. Foraminifera were poorly preserved and relative abundances were low, mainly composed of benthic taxa. A consistent assemblage is composed of calcareous benthic *Ammonia beccarii*, *Elphidium poeyanum*, and *Melonis barleeanum* (Additional file 4). There are poorly preserved planktonic foraminifera, including *Globoturborotalita* cf. *woodii* and *Globoturborotalita* cf. *rubescens* (Additional file 4). The assemblage also contains *Rhabdammina cylindrica* and *Gyroidinoides complanatus* from the early to middle Miocene or older (Bolli et al. 1994; Kaminski and Gradstein 2005) that could be considered as reworked.

Paleodiversity and taxonomy

A total of 1746 cranial and postcranial specimens represent the fossil sample from the San Gregorio Formation, 1719 specimens from the NCC locality (Vergel Member), while 27 are from SGOP locality (Cocuiza Member). Herein a terrestrial and freshwater faunal diversity of at least 49 taxa (fishes, amphibians, reptiles, and mammals) is reported from NCC (Fig. 31), including taxa previously described from the locality (Carlini et al. 2008c, 2018; Carlini and Zurita 2010; Vucetich et al. 2010; Zurita et al. 2011; Scheyer et al. 2013; Castro et al. 2014; Forasiepi et al. 2014; Carrillo et al. 2018). The terrestrial and freshwater vertebrate diversity reported for the first time from the SGOP locality includes nine reptilian and mammalian taxa (Fig. 31).

Chondrichthyes Huxley, 1880
Batomorphii Cappetta, 1980
Myliobatiformes Compagno, 1973
Potamotrygonidae Garman, 1877
Potamotrygon Garman, 1877
Potamotrygon sp.
(Fig. 4A1–J).

Locality: NCC (conglomerate, Fig. 3B).
Material: Fifty-two isolated teeth of indeterminate jaw position (AMU-CURS-868–875, -1094 and -1212) and 36 fragmented caudal spines (AMU-CURS-865).
General description, comparisons and remarks: The teeth are small, less than 2.4 mm wide, and 2 mm high. The crown is higher than the root, with a middle transverse crest that separates the labial and lingual sides. Two crown shapes are recognized, one with a cusp and the other without one. In the cuspidate teeth, the crest is lingually elongated and forms a distinctive triangular cusp; the labial side of most specimens is concave. In non-cuspidate teeth, the crown looks wider than long, with both rounded and concave labial sides. We identify the presence of teeth with cuspidate (males) or non-cuspidate (females) crowns, as the sexual dimorphism in adult individuals of the freshwater stingray *Potamotrygon* (see Adnet et al. 2014). With the exception of only two cuspidate teeth (Fig. 4G1–H3), remaining teeth are ornamented on their labial side. All specimens have a strongly convex lingual side. The root is a typical holaucorhize type, with two lobes having both rounded and flattened basal sections; a central foramen is present in the nutritive grove.

The caudal spines are eroded and broken (Fig. 4I, J); however, most of the specimens preserve their denticles, as well as the central ridge and central groove in the ventral and dorsal sides, respectively. The morphological characters present in the teeth and caudal spines from the NCC locality coincide with those present in *Potamotrygon* (e.g., Adnet et al. 2014 and references there in). Nevertheless, due to the scarce comparative material and the poor knowledge of the broader dental pattern among more than 30 recognized living *Potamotrygon* species from different South American river basins, we refrain from a more specific allocation.

Myliobatiformes indet.
(Fig. 4K1–K3).

Locality: NCC (conglomerate, Fig. 3B).
Material: An isolated vertebra (AMU-CURS-1213).

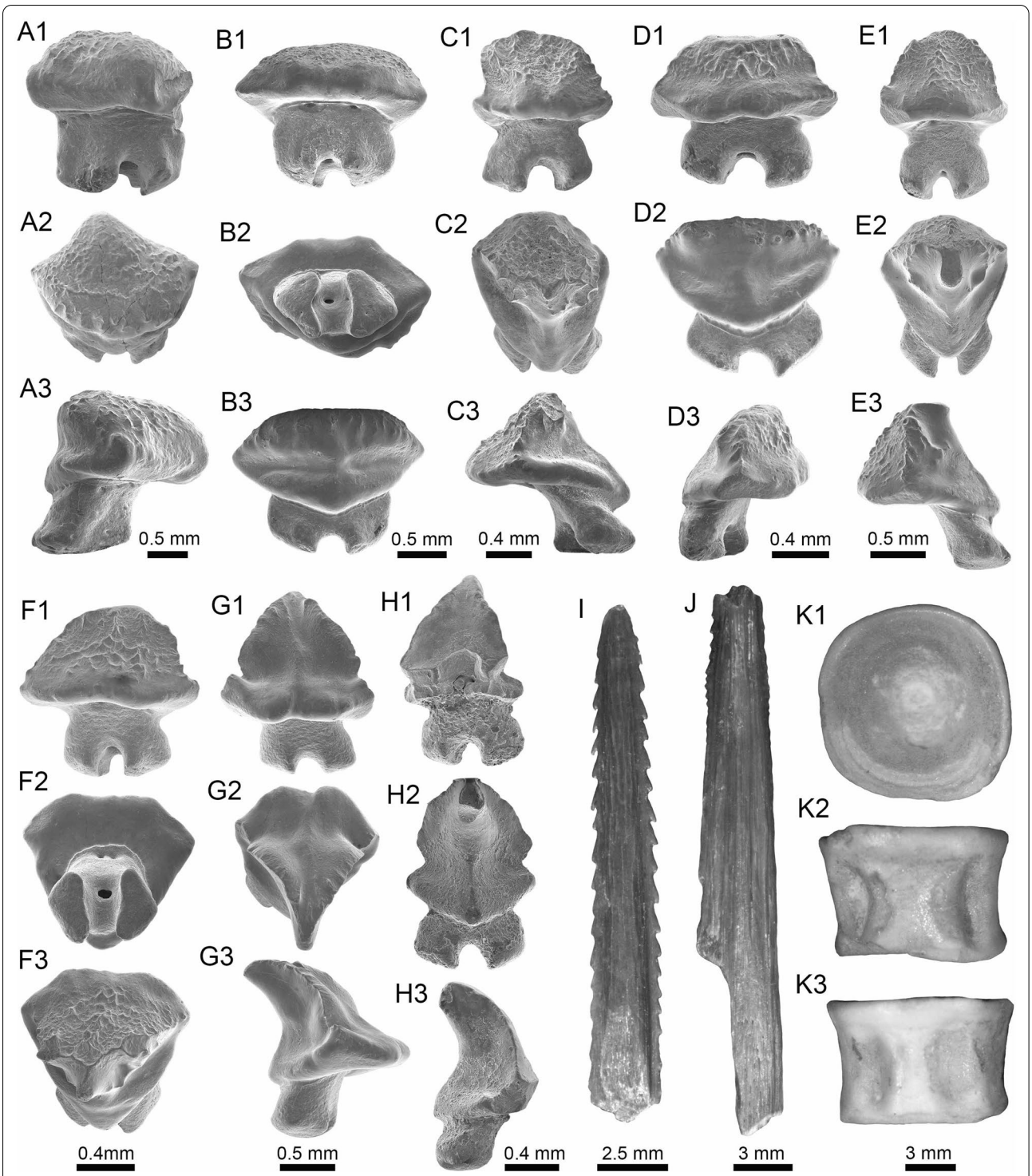

Fig. 4 Stingrays from the Vergel Member. **A1**–**J** *Potamotrygon* sp. (teeth **A1**–**B3** AMU-CURS-868; **C1**–**D3** AMU-CURS-869; **E1**–**F3** AMU-CURS-870; **G1**–**H3** AMU-CURS-871; and caudal spines **I**, **J** AMU-CURS-865). **K1**–**K3** Myliobatiformes indet. Views: labial (**A1**, **B1**, **C1**, **D1**, **E1**, **F1**, **G1**, **H1**), lingual (**B3**, **D2**, **H2**), occlusal (**A2**, **C2**, **E2**, **F3**, **G2**), lateral (**A3**, **C3**, **D3**, **E3**, **G3**, **H3**), basal (**B2**, **F2**), ventral (**I**, **J**), and indet. (**K1**–**K3**)

General description, comparisons and remarks: The vertebra is small with an amphicoelous centrum 3.5 mm in diameter and 2.7 mm wide. A pair of dorsal and ventral foramina where the neural and hemal arches were nested are preserved. The dorsal and ventral foramina are elongated and not well defined, a diagnostic feature of ray vertebrae (see Kozuch and Fitzgerald 1989). Although the only batoid recorded until now in the San Gregorio Formation is *Potamotrygon*, the vertebra does not preserve diagnostic elements to assign it to that taxon.

Actinopterygii Klein, 1885
Characiformes (sensu Fink and Fink, 1981)
Anostomidae Günther, 1864
Megaleporinus Ramirez et al., 2017
cf. *Megaleporinus* sp.
(Fig. 5A1–B3).

Locality: NCC (conglomerate, Fig. 3B).
Material: Two premaxillary symphyseal teeth (AMU-CURS-851).
General description, comparisons and remarks: Premaxillary symphyseal teeth of up to 3.9 mm in height and 2 mm wide. Both teeth are straight, with a massive unicuspid incisiform crown, a deep concave labial side, and a rounded and slightly irregular cutting edge. The teeth preserve at their lateral edges a contact surface for other premaxillary teeth. Among the Anostomidae, premaxillary symphyseal teeth with a massive unicuspid incisiform shape are characteristics of *Megaleporinus*, of which eleven species are recognized (Ramirez et al. 2017; Birindelli et al. 2020). In contrast, *Abramites*, *Anostomoides*, and *Leporinus* have compressed teeth with a mesial ridge and usually a single outstanding cusp, often accompanied by smaller lateral cusps in juveniles (see Birindelli et al. 2013; Assega and Birindelli 2019). Our comparisons suggest also that the specimens AMU-CURS-851 resemble the premaxillary symphyseal teeth of *Megaleporinus muyscorum* in size and morphology (Fig. 5C1, C2), the only trans-Andean species inhabiting the Magdalena River basin. However, given that comparisons with *Megaleporinus* species were not exhaustive, we prefer to keep the specimens from San Gregorio Formation in open nomenclature. These specimens from the NCC locality represent the first fossil record for this genus.

Schizodon Agassiz, in Spix and Agassiz, 1829
Schizodon corti Schultz, 1944
Schizodon cf. *S. corti*
(Fig. 5D1–O).

Locality: NCC (conglomerate, Fig. 3B).
Material: Seventy teeth from the premaxilla and dentary (AMU-CURS-849–850 and -1141).
General description, comparisons and remarks: Teeth are up to 3.6 mm in height and 1.5 mm wide. The premaxillary teeth (Fig. 5D1–I) are essentially straight, possessing three cusps, with a concave and convex shape in lingual and labial sides, respectively. Dentary teeth (Fig. 5J–O) are recurved and chisel shaped, with a concave and convex shape in lingual and labial sides, respectively. Symphyseal teeth bearing three cusps, and between two and three cusps in the second and third positions. Myers (1950) used dental morphology to diagnose most genera of the Anostomidae, as it was widely used method then (Winterbottom 1980; Garavello and Santos 2009; Ramirez et al. 2017). The genera *Anostomus*, *Pseudanos*, and *Petulanos* have compressed teeth (i.e., without mesial ridge) with three or four rounded cusps of similar size on the premaxilla and dentary (see Myers 1950; Winterbottom 1980). *Gnathodolus*, *Sartor*, and *Synaptolaemus* have compressed teeth with three weak cusps on the premaxilla, and four, three, or one (respectively) extremely elongated teeth on the dentary (Myers 1950). *Laemolyta* has compressed teeth with three to five rounded cusps of similar size on the premaxillary (similar to *Anostomus*, for example), and compressed teeth with a truncated cutting edge on the dentary (see Mautari and Menezes 2006). *Rhytiodus* and *Schizodon* also have compressed teeth, but with acute three to five cusps on the premaxilla and dentary. The other genera have teeth with a mesial ridge and usually a single outstanding cusp. Based on these comparisons, the fossil teeth described from the NCC locality are consistent with *Schizodon*. According to van der Sleen and Albert (2018), *Schizodon* is represented by at least 14 species in the cis-Andean basins, and the knowledge of their intraspecific dental variation is poorly known (Sidlauskas and Vari 2008). The only trans-Andean species is *Schizodon corti* (Fig. 5P–S), which inhabits the Lake Maracaibo basin (Rodríguez-Olarte et al. 2009). Given the locality of the fossil teeth, we herein tentatively identify them as belonging to cf. *S. corti*. Nevertheless, better comparisons are due once more comparative material is available. These specimens from the NCC locality represent the first fossil record for the genus *Schizodon*.

Erythrinidae Valenciennes, 1847
Hoplias Gill, 1903
Hoplias sp.
(Fig. 6A–F).

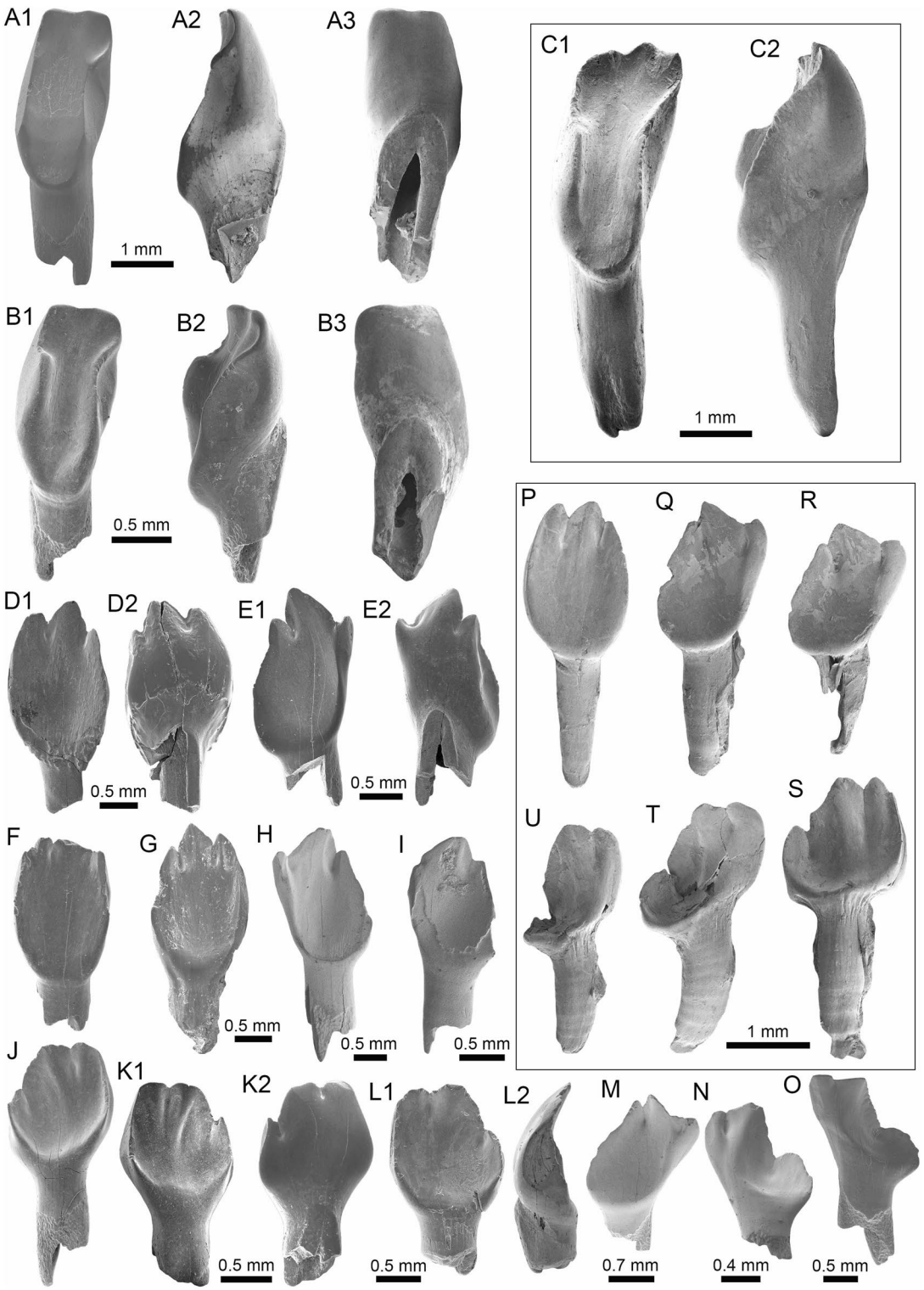

Fig. 5 Characiformes (Anostomidae) from the Vergel Member. **A1**–**B3** Premaxillary symphyseal teeth of cf. *Megaleporinus* sp. (AMU-CURS-851). **C1**, **C2** Recent premaxillary symphyseal tooth of *Megaleporinus muyscorum* (PIMUZ A/I 4856). **D1**–**O** *Schizodon* cf. *S. corti* teeth (**D1**–**G**, **J**–**L** AMU-CURS-849, and **H**, **I**, **M**–**O** AMU-CURS-849), of both premaxillary (**D1**–**I**) and dentary position (**J**–**O**). **P**–**U** Recent teeth of *Schizodon corti* (PIMUZ A/I 4869) [premaxillary (**P**–**R**) and dentary teeth (**S**–**U**), symphyseal teeth (**P** and **S**)]. Views: labial (**A3**, **B3**, **D2**, **E2**, **K2**), lingual (**A1**, **B1**, **C1**, **D1**, **E1**, **F-K1**, **L1**, **M-U**), and lateral (**A2**, **B2**, **C2**, **L2**)

Locality: NCC (conglomerate, Fig. 3B).

Material: Two hundred and forty-eight isolated teeth of indeterminate jaw position (AMU-CURS-824, -860, -1142 and -1215).

General description, comparisons and remarks: Teeth ranging up to 5.5 mm in height. These teeth are characteristics of homodont dentition, straight, or slightly curved with a conical and pointed shape. Crowns of pyramidal shape characterize the uppermost part of the teeth with distinctly sharp edges, and the basal portion is wider with a parallel sulcus. Half way up the crown, the tooth shows a narrowing or "waist" that separates the top of the crown from the base. The morphology of the specimens from the NCC locality is indistinguishable from that of the extant representatives of *Hoplias* (Fig. 6G1–I). Specific determinations are not possible with only isolated teeth.

Serrasalmidae Bleeker, 1859 (sensu Van Der Laan, 2018)

Mylossoma Eigenmann and Kennedy, 1903

Mylossoma sp.

(Fig. 6J1–N2).

Locality: NCC (conglomerate, Fig. 3B).

Material: Five complete symphyseal dentary teeth (AMU-CURS-1216).

General description, comparisons and remarks: The symphyseal teeth are up to 2.7 mm in height and up to 2 mm in width (Fig. 6J1–N2). The teeth are labiolingually and mesiodistally expanded, and have an oval base and smooth surfaces. In occlusal view, these are characterized by an ovoidal groove bordered by a labial transverse peaked crest and a lower lingual ridge. Other *Mylossoma* species within the "pacu clade" (see Thompson et al. 2014), such as *Colossoma* and *Piaractus*, also have a combination of molariform-like teeth adapted for crushing hard foods. Our comparative results suggest that teeth in adults are much smaller in *Mylossoma* than in *Colossoma* and *Piaractus*. The premaxillary and dentary teeth of the above-mentioned genera look very similar, especially those of *Colossoma* and *Piaractus,* which seem to be indistinguishable, hampering taxonomic identifications with isolated teeth. However, as it has been noticed by Dahdul (2004), and supported by our comparisons, fossil and recent symphyseal mandibular teeth, in both juveniles and adults of *Mylossoma*, *Colossoma*, and *Piaractus*, have a diagnostic concavity in the lingual face, in which the elevation of the distal edge is different among these genera. The *Mylossoma* specimens from the NCC locality differ from those of *Colossoma* and *Piaractus* and are practically indistinguishable from those of the extant species of *Mylossoma* (Fig. 6O1–P2), in which the symphyseal specimens are characterized by a narrow and low distal edge. Given that the morphology of AMU-CURS-1216 specimens is similar to both that of *Mylossoma acanthogaster*, the only trans-Andean species inhabiting the Lake Maracaibo basin (Rodríguez-Olarte et al. 2009) as well as to the other four recognized Cis-Andean species (Mateussi et al. 2018), more accurate specific identification for these specimens is not possible.

Serrasalmidae indet.

? "pacu clade."

(Figs. 6Q and 7A1–H).

Locality: NCC (conglomerate, Fig. 3B).

Material: Forty-two dentaries and premaxillary isolated teeth represent the sample (AMU-CURS-858–859 and -1143).

General description, comparisons and remarks: Teeth are up to 2.5 mm in height and 2 mm in width, although some broken and incomplete specimens could be larger. A molariform-like shape, being labiolingually and mesiodistally expanded with an oval base and a high crest, characterizes the teeth from the outer row (Fig. 7A1–D2). A molariform-like and elongated shape with a transverse and strongly peaked crest that is slightly curved to the lingual side, characterizes teeth from the inner row (Fig. 7E1–H). In all specimens, the transverse crest lacks serration. As previously mentioned, non-symphyseal mandibular teeth of the extant "pacu clade" (*Mylossoma*, *Colossoma* and *Piaractus*) look similar in shape across species. The specimens AMU-CURS-858–859 and AMU-CURS-1143 are comparable in morphology and size with the teeth of *Mylossoma*, the only representative of the "pacu clade" and Serrasalmidae so far registered for the Vergel Member. However, in our taxonomic comparisons we have been able to notice that non-symphyseal mandibular teeth of both *Colossoma* and *Piaractus* juveniles are comparable in size and morphology with those of *Mylossoma*. Added to this, other species of Serrasalmidae, especially some included in the "*Myleus* clade" (see Thompson et al. 2014), also have molariform-like teeth adapted for crushing hard foods (van der Sleen and Albert 2018). Thus, we neither allocate these isolated teeth to generic level nor discard that they could belong to more than one taxon within the "pacu" or "*Myleus*" clades.

Cichliformes Betancourt-R et al., 2013

Cichlidae Bonaparte, 1835

Cichlidae indet.

(Fig. 7I1–M2).

Locality: NCC (conglomerate, Fig. 3B).

Material: Ten complete and fragmented dorsal and anal fin spines (AMU-CURS-1223–1224).

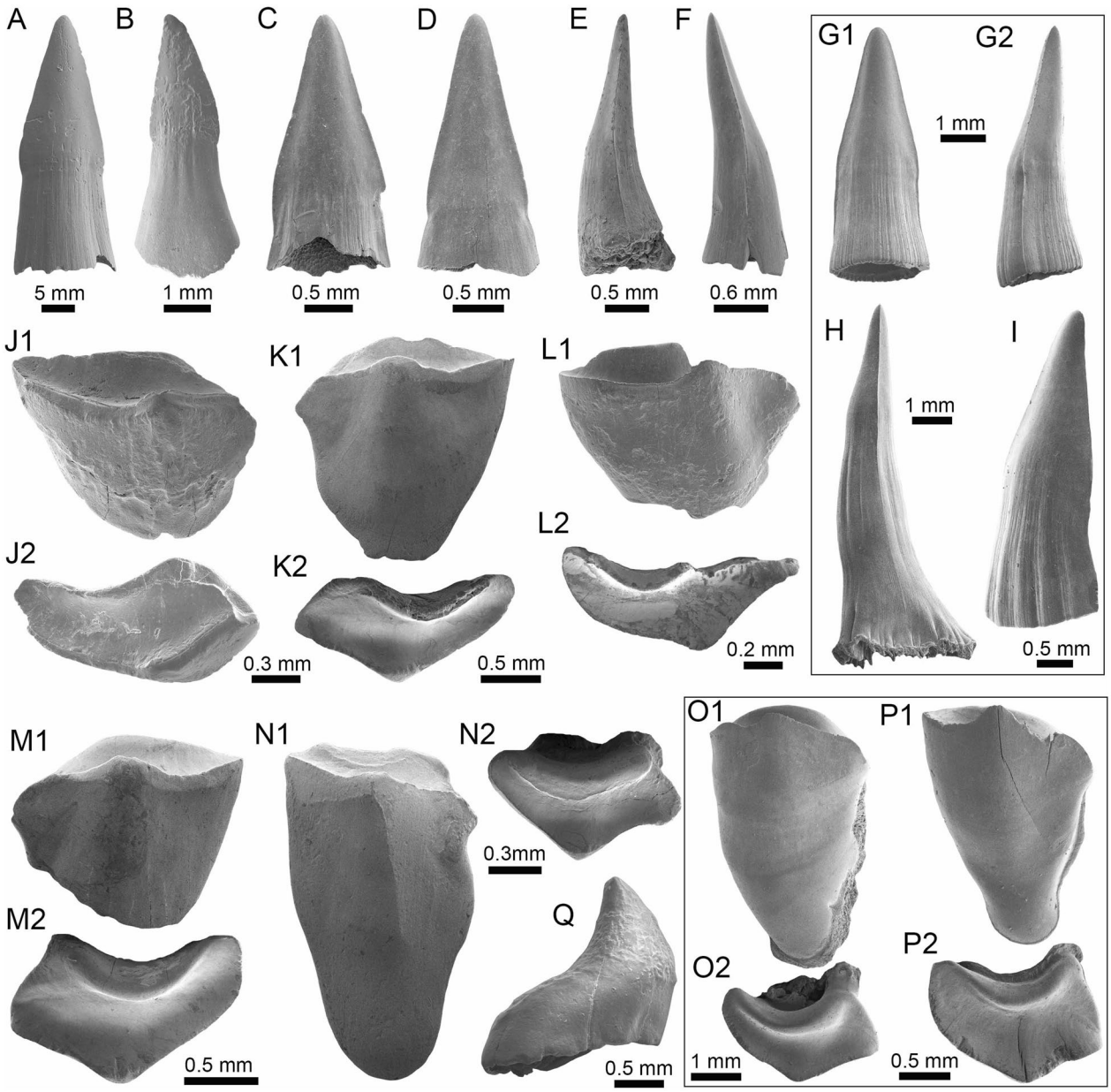

Fig. 6 Characiformes (Erythrinidae and Serrasalmidae) from the Vergel Member. **A**–**F** *Hoplias* sp. teeth of indeterminate position (**A**, **B** AMU-CURS-860 and **C**–**F** AMU-CURS-824). **G1**–**I** Recent teeth of *Hoplias malabaricus* (PIMUZ A/I 4875). **J1**–**N2** *Mylossoma* sp. symphyseal dentary teeth (AMU-CURS-1216). **O1**–**P2** Recent symphyseal dentary teeth of *Mylossoma albiscopum* (PIMUZ A/I 4860). **Q** Serrasalmidae indet. (? "pacu clade") dentary tooth (AMU-CURS-859). Views: labial (**A**, **D**, **I**, **J1**, **K1**, **L1**, **M1**, **N1**, **O1**, **P1**), lingual (**B**, **C**, **G1**), occlusal (**J2**, **K2**, **L2**, **M2**, **N2**, **O2**, **P2**), and lateral (**E**, **F**, **G2**, **H**, **Q**)

General description, comparisons and remarks: The only complete spine is 21 mm in length (Fig. 7J1–J3). The spines are robust and elongated, with a sharp end at the apical section. The anterior edge is smooth, the posterior one is characterized by a deep median grove, and the lateral sides are ornamented by parallel groves. A median foramen, lateral condyles, and posterior condylar process characterize the articular section of the spine. The specimens AMU-CURS-1223 have the typical morphology observed in dorsal and anal spines of cichlids. Nevertheless, it is difficult to make precise taxonomic identifications based on isolated spines. For this reason, these spines from Vergel Member cannot be referred to beyond indeterminate cichlids.

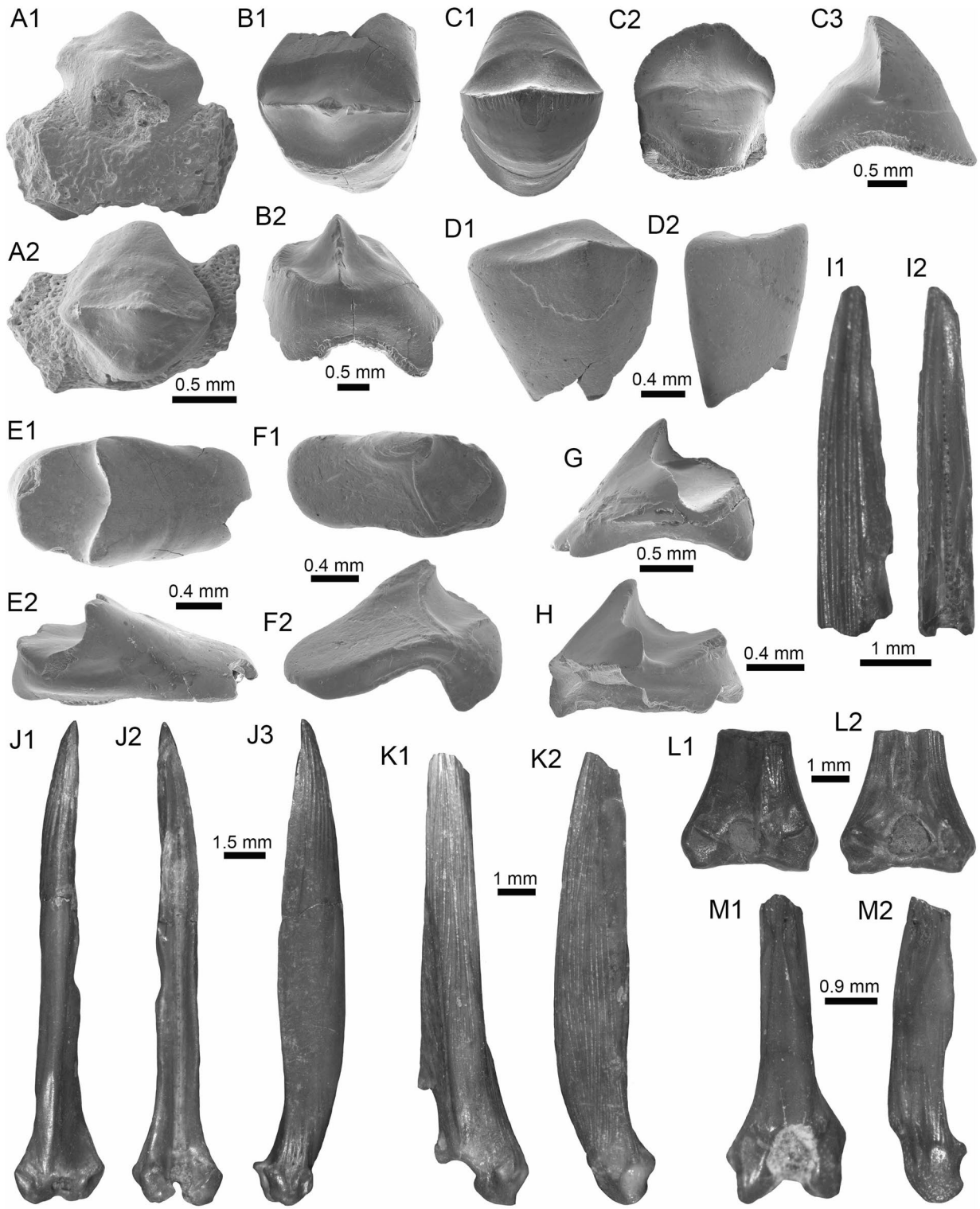

Fig. 7 Characiformes (Serrasalmidae) and Cichliformes from the Vergel Member. **A1**–**H** Serrasalmidae indet. (? "pacu clade"). **A1**–**D2** Molariform-like teeth from the outer row and **E1**–**H** from the inner row of indeterminate (dentary/premaxilla) position (**A1**, **A2** AMU-CURS-859 and **B1**–**H** AMU-CURS-858). **I1**–**M2** Dorsal (**J1**–**J3**, **M1**, **M2**), anal (**K1**, **K2**) and indeterminate position (**I1**, **I2**, **L1**, **L2**) fin spines of Cichlidae indet. (**I1**, **I2**, **L1**–**M2** AMU-CURS-1224 and **J1**–**K2** AMU-CURS-1223). Views: labial (**A1**, **D1**), lingual (**C2**), occlusal (**A2**, **B1**, **C1**, **E1**, **F1**), lateral (**B2**, **C3**, **D2**, **E2**, **F2**, **G**–**I1**, **J3**, **K2**, **M2**), anterior (**J1**, **K1**, **L1**, **M1**), and posterior (**I2**, **J2**, **L2**)

Siluriformes (sensu Grande, 1987)
Ariidae Bleeker, 1862
Sciades Müller and Troschel, 1849
cf. *Sciades* sp.
(Fig. 8A1–A3).

Locality: NCC (conglomerate, Fig. 3B).
Material: A fragmented dorsal spine (AMU-CURS-1058).
General description, comparisons and remarks: The spine is 22 mm in length, with only the anterior portion preserved. Most of the articular region is missing, preserving only part of the left lateral wing. The spine body is robust with a triangular shape in cross section (Fig. 8A1–A3) with lateral sides characterized by a striated ornamentation. A crest with thick tubercles and a posterior side with a deep groove characterize the body of the spine. The specimen AMU-CURS-1058 is closer in morphology to the dorsal spines of the extant species of *Sciades* (Fig. 8B1, B2) than to any other species of marine or freshwater catfish that we have been able to compare.

Callichthyidae Bonaparte, 1838
Callichthyidae indet.
(Fig. 8C1–G2).

Locality: NCC (conglomerate, Fig. 3B).
Material: Four pectoral-fin spine fragments, one left (AMU-CURS-1167a) and three of indeterminate position (AMU-CURS-1167b-1668), plus two bony plate fragments of the body armor (AMU-CURS-1169).
General description, comparisons and remarks: The two proximal pectoral-fin spines AMU-CURS-1167 are 11 and 13 mm in length, respectively; in both specimens, the articular process is missing. The shaft is ovoid in section, with the anterior and anterodorsal edges ornamented by small circular odontodes bases (Fig. 8C1, C2). The posterior edge preserves a strong dentation. Specimens AMU-CURS-1668 are ovoid in section and anterior and anterodorsally ornamented by small odontode bases and a well-developed dentation in the posterior edge (Fig. 8D1–E). Dorsal-fin spines anteriorly and anterodorsally ornamented by small odontodes and well-developed posterior dentitions are typical of Callichthyidae (Lundberg 1997). Although the bony plate fragments are incomplete (Fig. 8F–G2), an elongated shape with smooth surface can be observed, a feature that characterizes the body armor plates of the Callichthyidae taxa (e.g., van der Sleen and Albert 2018). Due to the absence of diagnostic characters in the specimens, the presence of more than a single taxon cannot be ruled out.

Doradidae Bleeker, 1858
Astrodoradinae Higuchi et al., 2007
Amblydoras Bleeker, 1862
cf. *Amblydoras* sp.
(Fig. 8H1–H3).

Locality: NCC (conglomerate, Fig. 3B).
Material: A partial left cleithrum (AMU-CURS-1225), including the nearly complete posterior cleithral process and its base.
General description, comparisons and remarks: The cleithrum is 14 mm in length and 6 mm in maximum height. The anterior portion, corresponding to the base of the posterior cleithral process, including part of the cleithrum bulge laterally, and part of the sulcus medially, where the dorsal articular process of the pectoral-fin spine inserts. Dorsal process of cleithrum partially preserved, immediately dorsal to the anterior portion of posterior process of cleithrum. Medial face of posterior process of cleithrum smooth and concave at base. Lateral face of posterior cleithral process concave at base and straight posteriorly, bearing a longitudinal series of aligned spines and a longitudinal keel immediately dorsal to the series of spines (Fig. 8H1–H3). Series of spines, including six small protuberances near base, from anteriormost portion to terminus of dorsal process, and posteriorly to that point, possessing six larger protuberances well spaced. Protuberances from 0.01 to 0.05 mm in height. Tip of posterior cleithral process straight and blunt. The presence of a series of well-spaced aligned spines in AMU-CURS-1225 distinguishes this fossil from most species of Doradidae, as this is a characteristic feature of Astrodoradinae (Higuchi et al. 2007; Birindelli 2014). Among Astrodoradinae, only *Amblydoras*, *Anadoras*, and *Astrodoras* possess relatively large, distinct well-spaced spines that are aligned on the posterior cleithral process. Of the three aforementioned genera, *Anadoras* and *Astrodoras* have the posterior cleithral process slightly deeper and more triangular than *Amblydoras*. Therefore, the AMU-CURS-1225 is most similar to *Amblydoras* (Fig. 8I1, I2). The specimen AMU-CURS-1225 from the Vergel Member represents the first fossil record for the genus *Amblydoras*.

Scorpiodoras Eigenmann, 1925
cf. *Scorpiodoras* sp.
(Fig. 8J1–J3).

Locality: NCC (conglomerate, Fig. 3B).
Material: A partial right cleithrum (AMU-CURS-1226), including exclusively the posterior half (or third) of the posterior cleithral process.

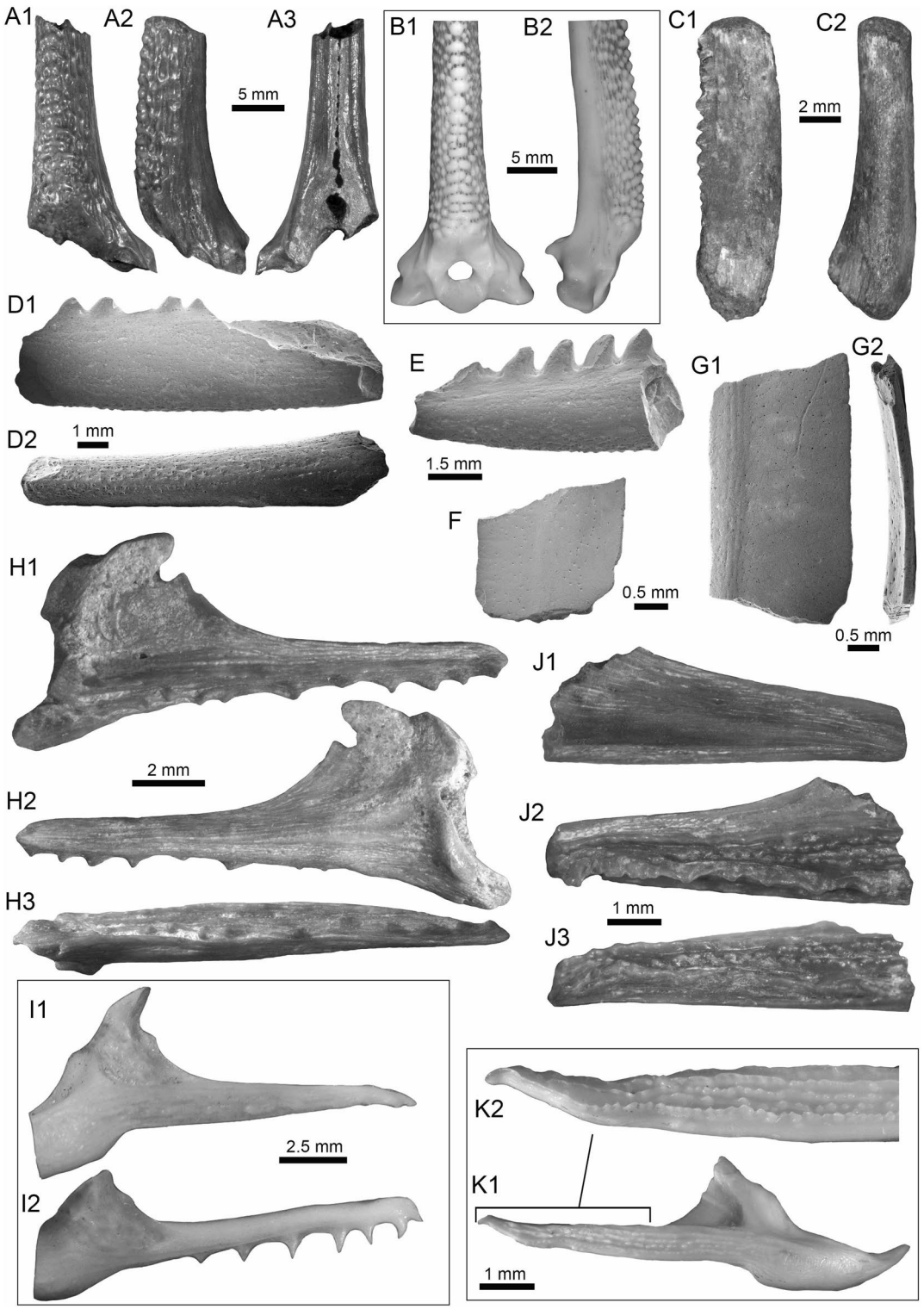

Fig. 8 Siluriformes (Ariidae, Callichthyidae, and Doradidae) from the Vergel Member. **A1**–**A3** Dorsal spine of cf. *Sciades* sp. (AMU-CURS-1058). **B1**, **B2** Recent dorsal spine of *Sciades proops* (PIMUZ A/I 4874). **C1**–**E** Pectoral-fin spines and **F**–**G2** bony plate fragments of Callichthyidae indet. (**C1**, **C2** left spine, AMU-CURS-1167a; **D1**–**E** AMU-CURS-1168 and **F**–**G2** AMU-CURS-1169). **H1**–**H3** Partial left cleithrum cf. *Amblydoras* sp. (AMU-CURS-1225). **I1**, **I2** Recent left cleithrum of *Amblydoras affinis* (CAS 66236). **J1**–**J3** Partial right cleithrum of cf. *Scorpiodoras* sp. (AMU-CURS-1226). **K1**, **K2** Recent left cleithrum of *Scorpiodoras heckelii* (MHNLS-17959). Views: anterior (**A1**, **B1**, **C2**, **D2**), dorsal (**C1**, **I2**), dorsolateral (**H1**, **J2**), lateral (**A2**, **B2**, **F**–**G1**, **H3**, **J3**, **K1**, **K2**), mesial (**J1**), posterior (**A3**), ventral (**H2**), and indet. (**D1**, **E**, **G2**)

General description, comparisons and remarks: AMU-CURS-1226 is approximately triangular in shape, with around 9 mm in length and 3 mm in maximum height. Anterior border convex with irregular margin, dorsal margin is concave and the ventral one straight. Posterior tip of process blunt. Medial face smooth. Lateral face ornamented with more or less six longitudinal ridges. Two dorsal most ridges, more or less continuous (i.e., not denticulated) and relatively short (approximately 0.01 mm of height). Next two longitudinal ridges (0.01 mm of height), from dorsal to ventral margins, denticulated and converging approximately at middle of the specimen. Fifth ridge (from dorsal to ventral margins) largest, approximately of 0.2 to 0.8 mm in height, more robust near tip of process and distinctly denticulated (or composed of coalescent distally oriented spines). Tip of posterior cleithral process somewhat tilted laterally. The presence of strong ridges (Fig. 8J2, J3), including a horizontal series of spines (even as denticulated ridges), distinguishes this fossil from most species of Doradidae, as this is a characteristic feature of Astrodoradinae (Higuchi et al. 2007; Birindelli 2014). The presence of denticulated longitudinal series and the distally curved posterior cleithral process is only present in *Scorpiodoras* (Fig. 8K1, K2). The specimen AMU-CURS-1226 assigned to cf. *Scorpiodoras* sp. from the NCC locality represents the first fossil for the genus.

Doradidae indet.
(Figs. 9A1–J and 10A1–I2).

Locality: NCC (conglomerate, Fig. 3B).

Material: An assortment of doradid remains, including three skull fragments (AMU-CURS-1170, -1227 and -1175), 62 pectoral (AMU-CURS-667, -1233–1234) and 11 dorsal spines (AMU-CURS-1180), and four mid-lateral scutes (AMU-CURS-864 and AMU-CURS-1232a-c).

General description, comparisons and remarks: AMU-CURS-1227 is a complete disarticulated parieto-supraoccipital (Fig. 9A1, A2). It is around 12 mm in length, 8 mm in width, and 3 mm in height. Nonagon shaped, with posterior margin straight (presumably sutured to anterior nuchal plate). Anterior margin pointed with contralateral concave margins (presumably sutures to frontals). Lateral margin composed of three stretches of concave margins, with width greater around last third of bone. Dorsal surface relatively flat and ornamented with small depressions, including two relatively parallel lines of depressions near the anterolateral tips (close to presumably suture between frontals and sphenotic). Ventral surface of bone with three concavities, one large covering most of the surface and two contralateral ones in the posterior portion, divided by a longitudinal bony septum. The truncated posterior margin in AMU-CURS-1227 leaves no doubt that the specimen belongs to either a Doradidae or an Auchenipteridae specimen. The relative flatness and the proportions (i.e., more elongated than wide) are more similar to features of Doradidae than to Auchenipteridae.

AMU-CURS-1170 is a partial parieto-supraoccipital, including possibly the middle of the bone (Fig. 9B). Specimen with approximately 9 mm in maximum width and 7 mm in length. Dorsal surface flat with some ornamentation composed of small depressions, including a part of the longitudinal line of depression linked to the sensory canal that runs from the parieto-supraoccipital to the frontals, and the transversal line of relatively larger depressions that runs in the middle of the parieto-supraoccipital. The flat parieto-supraoccipital bone is ornamented with small depressions, resembling the parieto-supraoccipital of Doradidae. It is likely that AMU-CURS-1227 and AMU-CURS-1170 belong to cf. *Amblydoras* sp. or cf. *Scorpiodoras* sp.; however, given the broken nature of the specimens and the small portion of diagnostic anatomy they preserve, we suggest an allocation at the family level.

AMU-CURS-1175 is a partial left cleithrum fragment, of around 7 mm in length and 7 mm in maximum height (Fig. 9C). Although the poor preservation of this specimen precludes a more precise taxonomic identification, its general morphology is somewhat different from that of the cleithrum of *Amblydoras* and *Scorpiodoras*. This suggests the presence of a third Doradidae taxon in the Vergel Member assemblage.

The pectoral-fin spines (AMU-CURS-667, -1233–1234) include fourteen right specimens, 16 left, and 30 of indeterminate position. The spines are broken (Fig. 9E1–J), and the most complete one is 29 mm in length (Fig. 9D1–D3). The shaft is robust, well ossified, and flattened dorso-ventrally, with an oval shape in cross section. Both dorsal and ventral surfaces of the shaft bear coarse parallel groves. The anterior edge is characterized by small triangular and sharp denticles, which are inclined in the distal direction. Denticles of the posterior edge are bigger than the ones on the anterior edge, and these are inclined toward the proximal direction of the spine. In the well-preserved articular sections, the dorsal articular process is semi-circular and wide, the articular groove is triangular and large, and the anterior and ventral processes are well developed. Dorsal-fin spines (AMU-CURS-1180) are also in fragmentary condition, preserving only the proximal-half portions (Fig. 10A1–D2); the most complete one is 13 mm in length. These are robust and triangular in cross section, with lateral sides characterized by coarse parallel groves. In most specimens, the dorsal section is smooth, but two of the specimens bear triangular denticles inclined distally. The articular region is triangular with a prominent anterior process, a circular articular foramen, and a well-developed medial process. These fossil pectoral-fin and dorsal-fin spines resemble those of the extant species of *Amblydoras*, *Scorpiodoras*, *Anadoras* (e.g., Figs. 9K1–L3

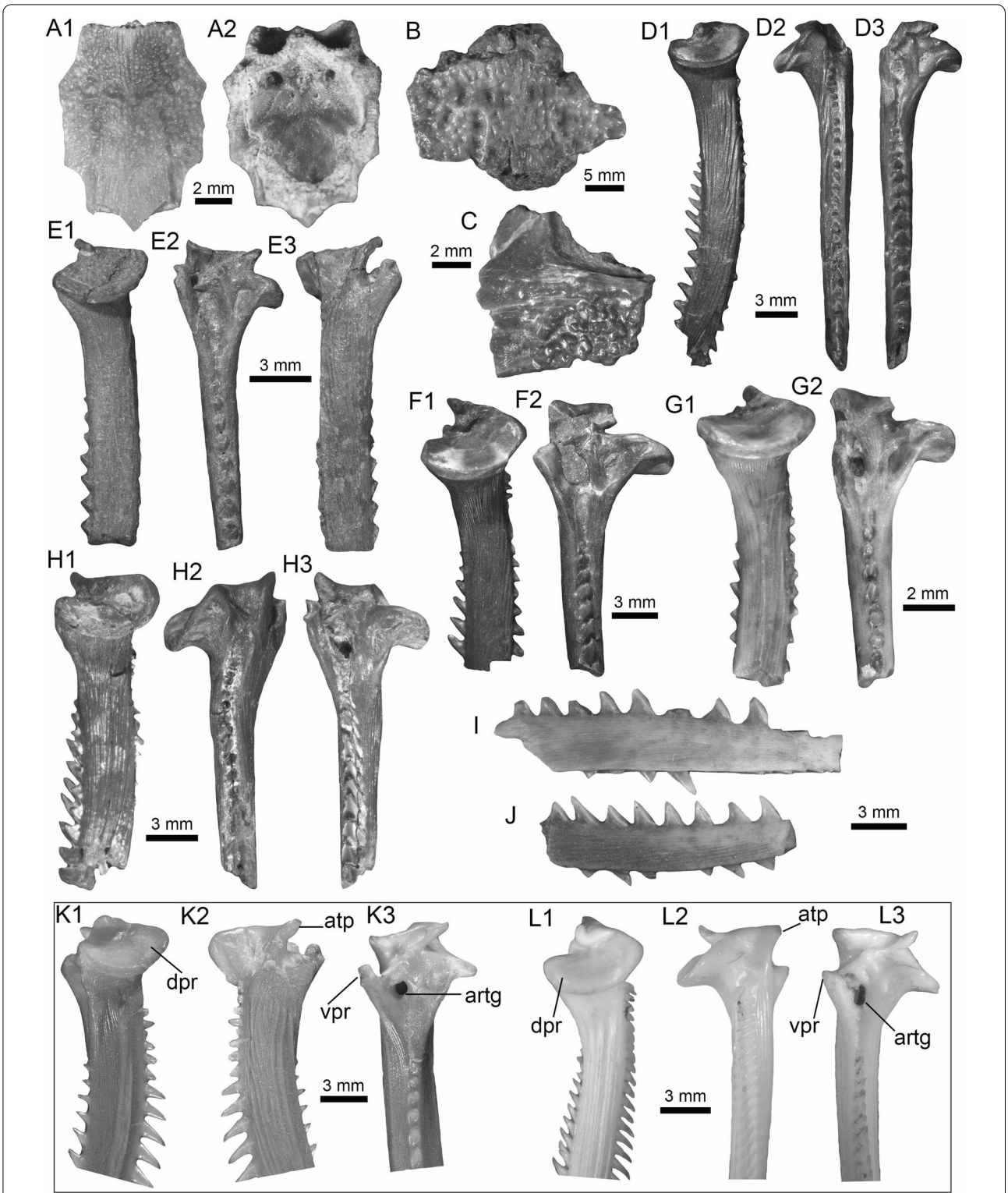

Fig. 9 Siluriformes (Doradidae) from the Vergel Member. **A1**–**J** Doradidae indet. **A1**, **A2** Parieto-supraoccipital (AMU-CURS-1227). **B** Partial parieto-supraoccipital (AMU-CURS-1170). **C** Partial left cleithrum (AMU-CURS-1175). **D1**–**J** Pectoral-fin spines (**D1**–**H3** AMU-CURS-1234 and **I**, **J** AMU-CURS-1233), position: right (**D1**–**H3**) and indet. (**I**, **J**). **K1**–**L3** Right pectoral-fin spines of extant *Anadoras wedellii* (**K1**–**K3** AUM-45441) and *Scorpiodoras heckelii* (**L1**–**L3** MHNLS-17959). Views: anterior (**D2**, **H2**, **L2**), dorsal (**A1**, **B**, **C**, **D1**, **E1**, **F1**, **G1**, **H1**, **K1**, **L1**), posterior (**D3**, **E2**, **F2**, **G2**, **H3**, **K3**, **L3**), ventral (**A2**, **E3**, **K2**), and indet. (**I**, **J**). *atp* anterior process, *artg* articular grove, *dpr* dorsal process, *vpr* ventral process

and 10E1–F3), and other members of Astrodoradinae. However, due to the fragmentary and poor preservation of most of the specimens, added to the poor knowledge of intraspecific spine variation in Doradidae catfishes, determinations that are more accurate are not possible.

The partial mid-lateral scute (AMU-CURS-864a) is 1.5 mm in length (thorn length), preserving the entire thorn and its base (Fig. 10G). The thorn is strongly curved and posteriorly oriented. AMU-CURS-864b is also a partial mid-lateral scute of approximately 0.5 mm in length, preserving only part of the thorn near its base (Fig. 10H). The thorn is curved, posteriorly oriented, with a relatively small base (likely smaller than half of thorn). AMU-CURS-1232a-b correspond to two mid-lateral scutes. One of the specimens (AMU-CURS-1232a) is partially preserved (right body side), with length approximately 1.2 mm and height around 0.6 mm (Fig. 10I1, I2). AMU-CURS-1232b is a mid-lateral scute thorn completely preserved, posteriorly oriented, with distal margin convex, base larger than half of thorn (measured from anterior insertion of base to posterior tip). Doradidae are the only catfishes bearing mid-lateral scutes with a posteriorly oriented thorn. However, due to the fragmentary nature of the specimens, an identification to generic level is impossible. In any case, the mid-lateral scutes of the caudal peduncle usually possess elongated thorns, whereas the mid-lateral scutes on the center of the body usually possess smaller thorns with relatively large bases.

Heptapteridae Gill, 1861
Pimelodella Eigenmann and Eigenmann, 1888
cf. *Pimelodella* sp.
(Fig. 10J).

Locality: NCC (conglomerate, Fig. 3B).

Material: One incomplete pectoral-fin spine of indeterminate position, 6.5 mm in length (AMU-CURS-1183).

General description, comparisons and remarks: The specimen corresponds to the distal part of the spine, with a well-ossified and compressed shaft of sub-rectangular shape in cross section. Both dorsal and ventral surfaces of the shaft exhibit parallel shallow grooves and small pits. The anterior edge of the spine is characterized by small triangular denticles inclined toward distal direction where they become progressively smaller. The most distal section of the anterior edge (apical section) lacks denticles. In contrast, denticles in the posterior edge tend to be lightly inclined toward the proximal direction of the spine, and are wider, larger, and better defined than the denticles of the anterior edge. Although in AMU-CURS-1183 the articular section is missing, the combination of the above-mentioned characters supports the specimen's assignment within Heptapteridae. AMU-CURS-1183 is tentatively assigned to cf. *Pimelodella*, whose pectoral spines in fossil and extant species are characterized by an ornamentation pattern that can be clearly differentiated from other Siluriformes genera (Bisbal and Gómez 1986; Lundberg and McDade 1986; Bogan et al. 2020).

Loricariidae Rafinesque, 1815
Hypostominae Kner, 1853
Hypostominae indet.
(Fig. 10K1–P).

Locality: NCC (conglomerate, Fig. 3B).

Material: Nine pectoral-fin spine fragments (AMU-CURS-817 and -1173), and three isolated odontodes (AMU-CURS-876).

General description, comparisons and remarks: Pectoral-fin spine fragments of up to 15 mm in length (Fig. 10K1–N2). The three isolated and elongated odontodes are up to 3 mm in length (Fig. 10O, P). In the pectoral-fin spines, the articular region is missing, and only one fragmentary anterior section is preserved. The shaft of the spines is robust, slightly flattened dorso-ventrally with an oval cross section; only the two largest specimens preserve the articular groove, which is elongated in outline. Small circular odontode bases ornament the anterior and anterodorsal section. Parallel low ridges characterize the dorsal surface, forming grooves with small circular odontode bases; a well-developed line of circular odontode bases is present along the posteriodorsal edge. In the posterior margin of the shaft, a longitudinal sulcus is present. Pectoral spines bearing well-developed odontodes could be a representative character of Hypostominae, contrary to other loricariids subfamilies where the pectoral spine is always with thick skin or dermal plates (e.g., van der Sleen and Albert 2018). AMU-CURS-1173 resembles the shaft of *Hemiancistrus*; nevertheless, the fragmentary condition limits further recognition of more than one taxon and the taxonomic assignment beyond Hypostominae.

Loricariidae indet.
(Fig. 10Q, R).

Locality: NCC (conglomerate, Fig. 3B).

Material: Four body plates of the body armor (AMU-CURS-1230) and five broken and eroded small articulate sections of pectoral spines (AMU-CURS-1231).

General description, comparisons and remarks: Three of the body armor plates are fragmented and of indeterminate position; the complete specimen is 2.7 mm wide (Fig. 10Q) and presumably corresponds to a plate of the median position. Both the complete and the fragmented plates are ornamented by parallel rows of odontodes forming keels. Loricariids belong to a diverse group of

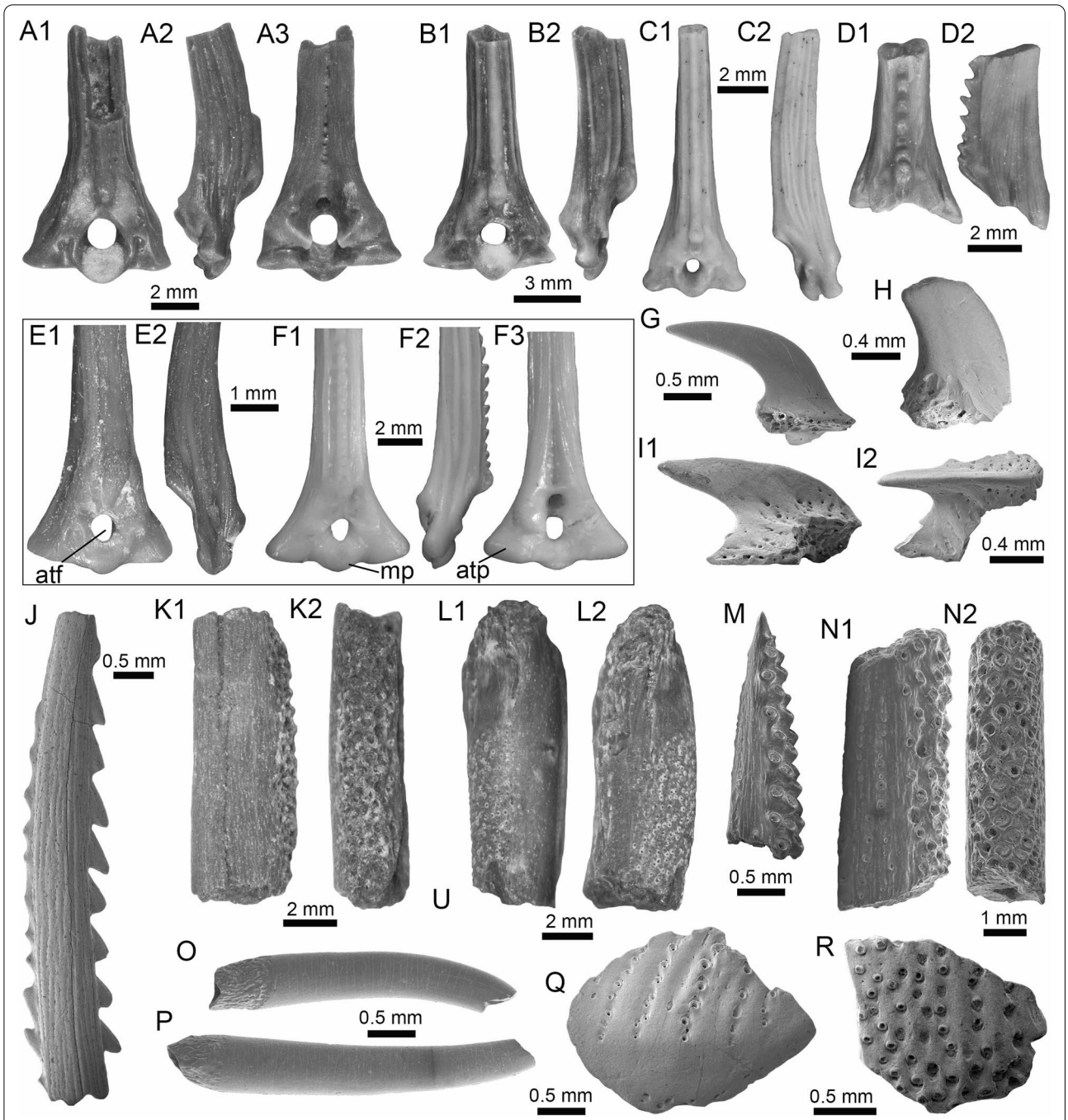

Fig. 10 Siluriformes (Doradidae, Heptapteridae, and Loricariidae) from the Vergel Member. **A1**–**D2**, **G**–**I2** Dorsal-fin spines (**A1**–**D2** AMU-CURS-1180) and mid-lateral scutes (**G**, **H** AMU-CURS-864a-b and **I1**, **I2** AMU-CURS-1232a) of Doradidae indet. **E1**–**F3** Dorsal spines of extant *Anadoras wedellii* (**E1**, **E2** AUM-45441) and *Scorpiodoras heckelii* (**F1**–**F3** MHNLS-17959). **J** Pectoral spine of cf. *Pimelodella* sp. (AMU-CURS-1183). **K1**–**P** Pectoral spine fragments (**K1**–**I2** AMU-CURS-1173 and **M**–**N2** AMU-CURS-817), and odontodes (**O**, **P** AMU-CURS-876) of Hypostominae indet. **Q**, **R** Body plates of Loricariidae indet. (AMU-CURS-1230). Views: anterior (**A1**, **B1**, **C1**, **D1**, **E1**, **F1**, **K2**, **L1**, **N2**), lateral (**A2**, **B2**, **C2**, **D2**, **E2**, **F2**, **I2**, **O**–**P**) posterior (**A3**, **F3**), and indet. (**G**–**I1**, **J**, **K1**, **L2**, **M**, **N1**, **Q**–**R**). *atp* anterior process, *atf* articular foramen, *mp* medial process

armored Siluriformes (van der Sleen and Albert 2018), and taxonomic identification based on their isolated body plates is a difficult task. The fragmentary condition of the specimens limits further taxonomical recognition, especially to differentiate whether these materials also belong to the above-mentioned Hypostominae loricariids or not.

Pimelodidae (sensu Lundberg and Littman, 2003)
Platysilurus Haseman, 1911
cf. *Platysilurus* sp.
(Fig. 11A1–B3).

Locality: NCC (conglomerate, Fig. 3B).
Material: Three incomplete left pectoral spines (AMU-CURS-1172).
General description, comparisons and remarks: The specimens are up to 14 mm in length, preserving part of the shaft and the articular region (Fig. 11A1–B3); these are slightly curved, robust, and flattened dorso-ventrally with an oval cross section. Most of the spines preserve the dorsal articular process, which is robust and somewhat rectangular in shape; the anterior process is preserved only in two of the specimens, and the ventral process is missing. The articular groove is triangular in outline. Both dorsal and ventral surfaces of the shaft bear coarse subparallel grooves, and the anterior and posterior edges have small triangular denticulations. AMU-CURS-1172 are morphologically more similar to the dorsal and pectoral spines of the two extant species of *Platysilurus* (Fig. 11C1–C3) (for species diversity see van der Sleen and Albert 2018) than any other species of marine or freshwater catfish that we have been able to compare. However, due the poor preservation of the spines, we tentatively assign AMU-CURS-1172 specimens to cf. *Platysilurus*.

Pimelodidae indet.
(Fig. 11D1–E3).

Locality: NCC (conglomerate, Fig. 3B).
Material: Two incomplete right and left pectoral spines (AMU-CURS-1228).
General description, comparisons and remarks: The most complete spine reaches 25 mm in length (Fig. 11E1–E3). In both spines, the articular region is present. However, the dorsal process is eroded and broken in one of the specimens; anterior and ventral processes are missing. The shaft is flattened and slight curved, with parallel and longitudinal grooves. The anterior edge is characterized by small denticles inclined toward distal direction; in contrast, the posterior edge has bigger triangular denticles inclined toward the proximal direction of the spine. AMU-CURS-1228 resembles the pectoral spines of extant and fossil species of *Pimelodus* (see Lundberg 1997; Vallone et al. 2017) more than any other pimeloid species that we could compare. However, due to the fragmentary condition of AMU-CURS-1228, we prefer to tentatively assign them to Pimelodidae indet. Clear morphological differences between the spines AMU-CURS-1172 assigned to cf. *Platysilurus* (Fig. 11A1–B3) and AMU-CURS-1228 unequivocally support the presence of at least two pimeloids in the NCC assemblage.

Siluriformes indet.
(Fig. 11F–M).

Locality: NCC (conglomerate, Fig. 3B).
Material: Ninety-nine cranial and postcranial isolated elements, most of them in eroded and fragmentary condition that does not permit a confident identification beyond Siluriformes indet.
General description, comparisons and remarks: The sample includes a fragment of a left post-temporal and two other skull fragments of indeterminate position (AMU-CURS-1175, Fig. 11G, H), a precaudal vertebrae with a centrum of 10 mm wide and 8.3 mm high (AMU-CURS-1174, Fig. 11I1, I2), and 95 pectoral and dorsal spine fragments (AMU-CURS-867, and -1180–1183, Fig. 11J–M). Although shaft fragments represent most of the dorsal and pectoral spines, some eroded articular regions have also been identified in the sample (Fig. 11K). These dorsal and pectoral catfish spines are in a bad fragmentary state with a marked degree of erosion preventing the recognition of diagnostic elements that could allow taxonomic identification even at the family level. The specimen AMU-CURS-1237 is a partial left cleithrum with around 8.5 mm in length (Fig. 11F) whose general morphology and ornamentation suggests clear differences with cleithrum bones of the extant specimens of Ariidae, Callichthyidae, Doradidae, Heptapteridae, and Loricariidae taxa described above from the NCC assemblage (Table 1). AMU-CURS-1237 could belong to another taxon, probably to a pimeloid catfish. However, future new fossil specimens would be necessary to clarify its taxonomy.

Synbranchiformes (sensu Gosline, 1983)
Synbranchidae Swainson, 1838
Synbranchus Bloch, 1795
Synbranchus sp.
(Fig. 12A1–J).

Locality: NCC (conglomerate, Fig. 3B).
Material: One right and two left fragmented dentaries (AMU-CURS-1146-a-c), a pharyngeal bone (AMU-CURS-1146-d), and 15 isolated vertebrae (AMU-CURS-1171).
General description, comparisons and remarks: The fragmented dentaries (Fig. 12A1–C3) are between 2 and 3.5 mm long, preserving only their anterior-symphyseal

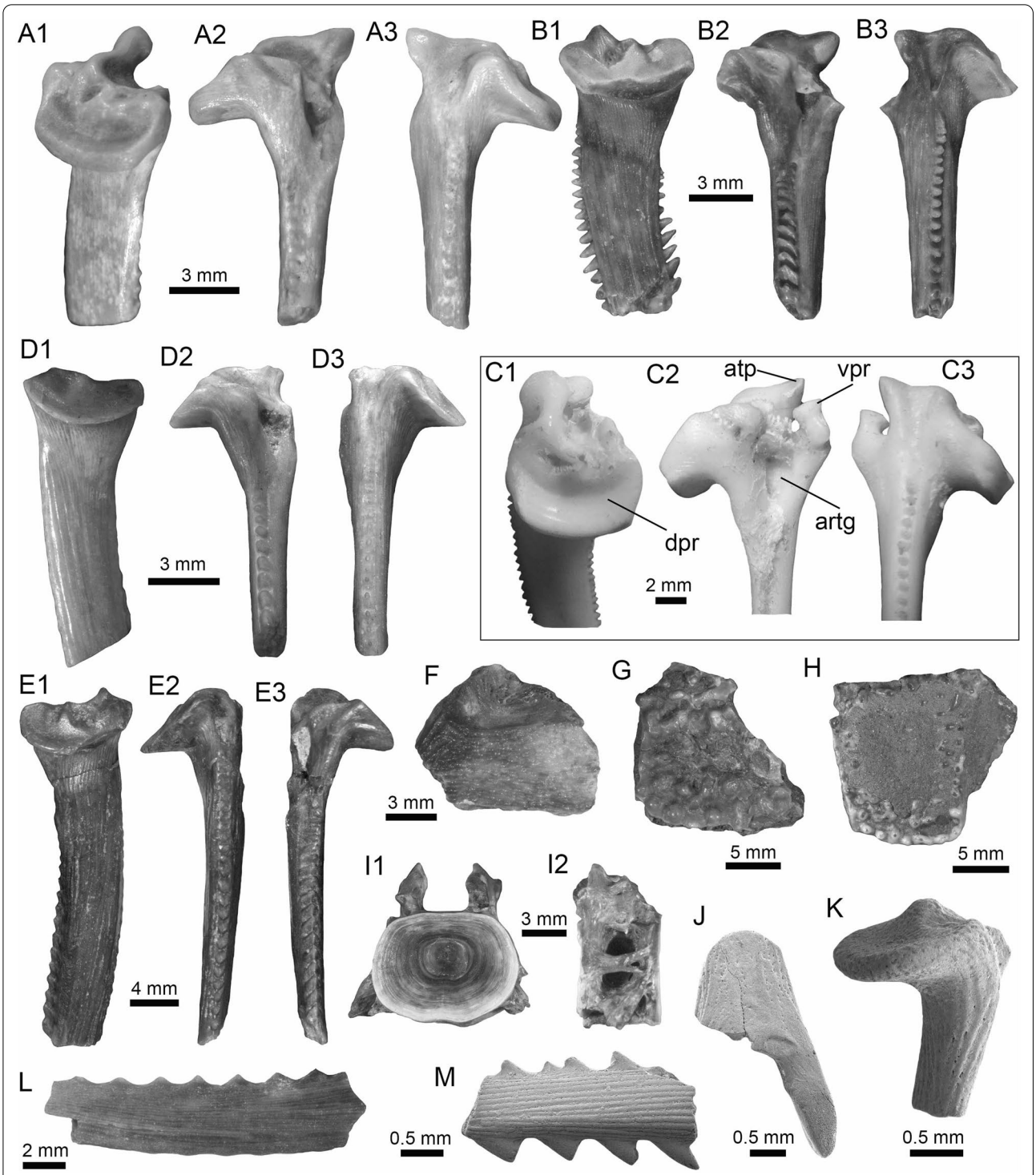

Fig. 11 Siluriformes (Pimelodidae and indet.) from the Vergel Member. **A1**–**B3** Left pectoral spines of cf. *Platysilurus* sp. (AMU-CURS-1172). **C1**–**C3** Left pectoral spine of extant *Platysilurus malarmo* (ANSP 187009). **D1**–**E3** Left (**D1**–**D3**) and right (**E1**–**E3**) pectoral spines of Pimelodidae indet. (AMU-CURS-1228). **F**–**M** Partial left cleithrum (**F** AMU-CURS-1237), skull fragments (**G**, **H** AMU-CURS-1175), precaudal vertebra (**I1**, **I2** AMU-CURS-1174), first dorsal spine (**J** AMU-CURS-1181), right pectoral spines (**K** AMU-CURS-867), and pectoral spine fragments (**L** AMU-CURS-867 and **M** AMU-CURS-1229) of Siluriformes indet. Views: anterior (**A3**, **B3**, **C3**, **D3**, **E2**, **I1**, **J**), lateral (**I2**), posterior (**A2, B2**, **C2**, **D2**, **E3**), dorsal (**A1**, **B1**, **C1**, **D1**, **E1**, **F**), anterodorsal (**K**), and indet. (**G**, **H**, **L**, **M**). *atp* anterior process, *artg* articular grove, *dpr* dorsal process, *vpr* ventral process

section. The anterior margin of the symphyseal region is rounded, exhibits a well-developed process, and the dorsal margin is covered by high subcircular tooth implantations. On the external face of each dentary, next to the symphyseal region, two well-developed foramina are observed. The pharyngeal bone (Fig. 12D1, D2) is 3 mm long, triangular, and covered by subcircular tooth implantations.

Most of the vertebrae are eroded and incomplete (Fig. 12G1–J), corresponding to six precaudal, three caudal, and one of indeterminate position. Precaudal vertebrae are characterized by a central body with the anterior face practically flat or slightly concave, and the posterior face wider than the anterior with a deep conical cavity; the transverse process is wide and ventrolaterally projected. Caudal vertebrate are not well preserved. However, like the anterior ones, a flat or slightly concave face characterizes the central body; the anterior face is bigger than the anterior, with a deep conical cavity, features that are characteristics in the vertebrate of Synbranchidae (Bogan et al. 2012). The fossil dentaries AMU-CURS-1146-a-c resemble those of the extant *Synbranchus marmoratus* (Fig. 12E1–F2), and their size suggests that these fossils would be fragments of small-sized individuals. Due to the poor preservation of the fossil dentaries, the lack of diagnostic elements in the isolated vertebrae, as well as the scarce osteological comparative material for some of the recognized living species of *Synbranchus*, especially those from the Amazon basin (see Utsunomia et al. 2014), a more accurate specific determination is not possible. The *Synbranchus* specimens from the NCC locality represent the oldest fossil record for this genus, since its fossil record was restricted to the Late Pleistocene of Argentina (Bogan et al. 2012).

Actinopterygii indet.
(Fig. 13A–Q).

Locality: NCC (conglomerate, Fig. 3B).

Material: Abundant isolated elements that include seven pharyngeal teeth (AMU-CURS-1145) and 12 other teeth of indeterminate position (AMU-CURS-1178). One hundred twenty-four complete and fragmented vertebrae of the precaudal and caudal regions (AMU-CURS-1176–1177 and -1240–1241). Forty-two fragmented cranial and postcranial bones (AMU-CURS-1179 and -1238) and 10 scale fragments (AMU-CURS-1863).

General description, comparisons and remarks: The isolated teeth are up to 2 mm in height (Fig. 13A–D). The poorly preserved cranial and postcranial bones (Fig. 13E, F) and scales (Fig. 13N–Q), lack diagnostic elements that allow a more detailed taxonomic assignment. In the case of the vertebrae, only a few specimens are complete (e.g., Fig. 13L1, L2). The rest of the specimens are incomplete and in a very poor preservational state, particularly in most of the vertebral centra. The largest vertebra in the sample does not exceed 4.5 mm in length (Fig. 13G–M). Given the small size of the vertebrae, they could belong to juveniles or other small-sized species, different from the taxa that can be recognized for the NCC assemblage (Table 1). Due to the poor preservation of the vertebrae and the scarcity of recent comparative material, a more detailed taxonomic identification is not possible at this time.

Lissamphibia Haeckel, 1866
Anura Fischer von Waldheim, 1813
Pipidae Gray, 1825a
Pipa Laurenti, 1768
cf. *Pipa* sp.
(Fig. 14A1, A2).

Locality: NCC (conglomerate, Fig. 3B).

Material: An incomplete sacral vertebra fused to a partial urostyle (AMU-CURS-722).

General description, comparisons and remarks: AMU-CURS-722 (total length 3.7 mm) preserves the vertebral centrum with a portion of the urostyle and poorly preserved transverse processes and prezygapophyses (a significant remnant of the right prezygapophyseal facet but much less of the left). Although the compound element is incomplete and moderately damaged, it clearly shows a single anterior condyle, planar diapophyses, a sacral sagittal dorsal ridge, and broad spinal foramina (one per side), which are useful characters for referring AMU-CURS-722 to pipids such as cf. *Pipa* sp. (see Delfino and Sánchez-Villagra 2018 and references therein). The specimen AMU-CURS-722 must have belonged to an individual of small size and the absence of a ridge on the sacral transverse process (there is only a hint of a very weak, elongated convexity directed posterolaterally) resembles characters present in *Pipa parva* (Fig. 14B1, B2) which is currently present in Falcón State (Mijares-Urrutia and Arends 2000). However, the poorly preserved condition of the specimens precludes a taxonomic identification beyond generic level.

Anura indet.
(Fig. 14C1–L).

Locality: NCC (conglomerate, Fig. 3B).

Material: The specimens correspond to 20 isolated and fragmented cranial and postcranial microelements that, due to their poorly preserved condition and lack of

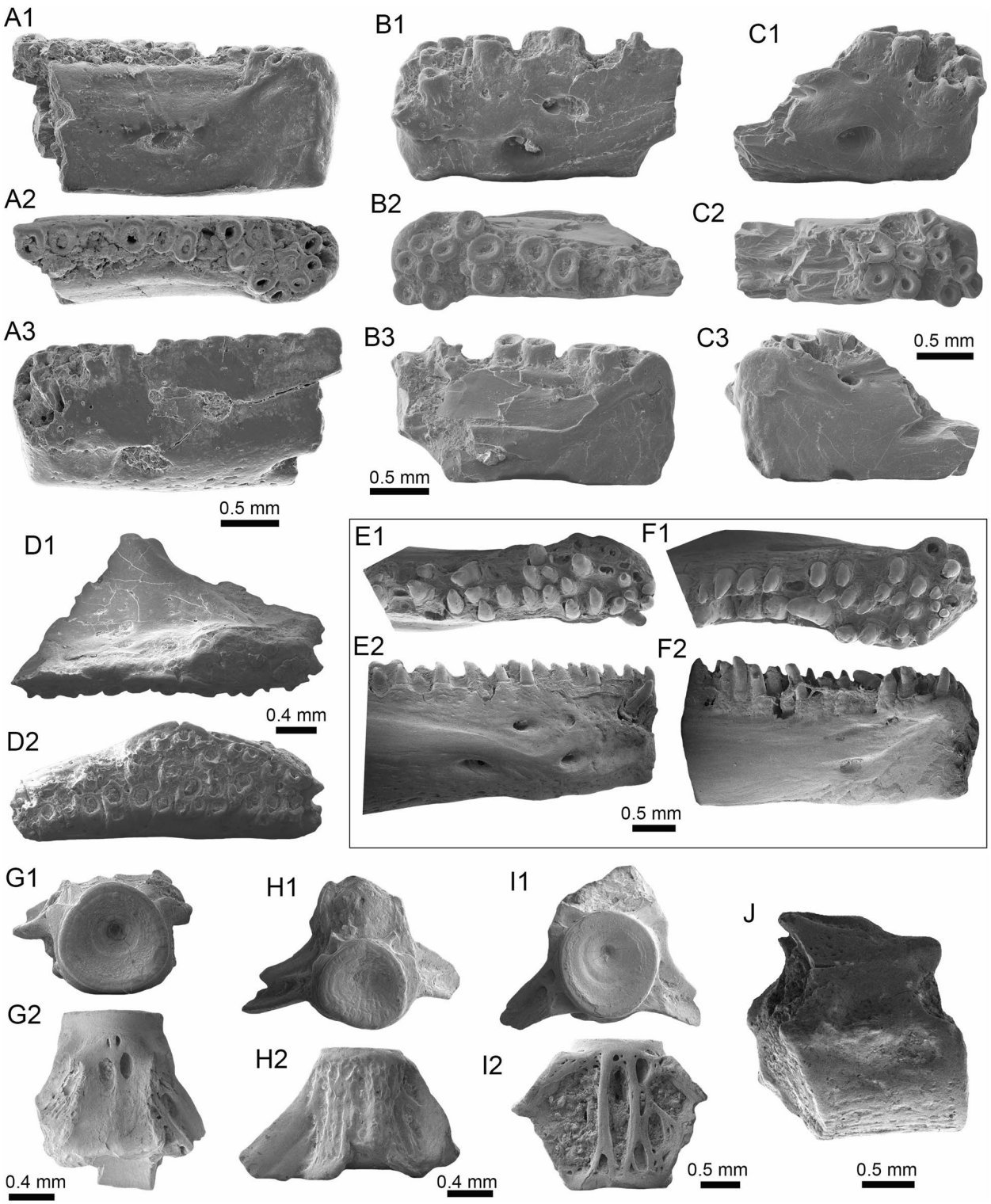

Fig. 12 *Synbranchus* sp. from the Vergel Member. **A1**–**C3** Dentaries (right: **A1**–**A3**, **C1**–**C3**, and left: **B1**–**B3**; AMU-CURS-1146-a-c) and branchial bones (**D1**, **D2** AMU-CURS-1146-d). **E1**–**F2** Right (**E1**, **E2**) and left (**F1**, **F2**) dentaries of extant *Synbranchus marmoratus* (PIMUZ A/I 4873). **G1**–**J** Isolated vertebrae of *Synbranchus* sp. (AMU-CURS-1171). Views: anterior (**G1**, **H1**, **I1**), left lateral (**B1**), right lateral (**A1**, **C1**, **E2**), lateral (**D1**, **J**), medial (**A3**, **B3**, **C3**, **F2**), occlusal (**A2**, **B2**, **C2**, **E1**, **F1**), and ventral (**D2**, **G2**, **H2**, **I2**)

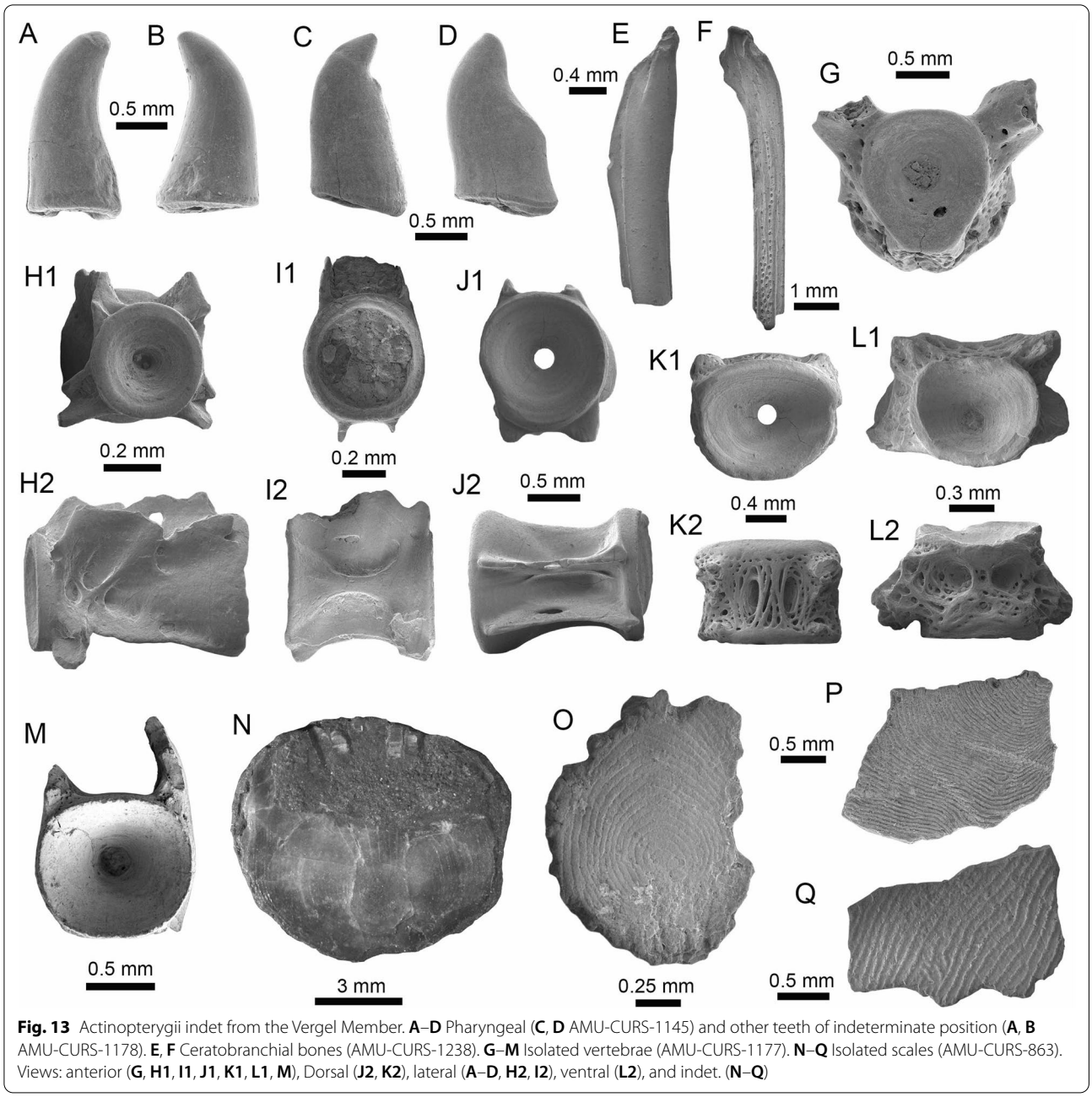

Fig. 13 Actinopterygii indet from the Vergel Member. **A**–**D** Pharyngeal (**C**, **D** AMU-CURS-1145) and other teeth of indeterminate position (**A**, **B** AMU-CURS-1178). **E**, **F** Ceratobranchial bones (AMU-CURS-1238). **G**–**M** Isolated vertebrae (AMU-CURS-1177). **N**–**Q** Isolated scales (AMU-CURS-863). Views: anterior (**G**, **H1**, **I1**, **J1**, **K1**, **L1**, **M**), Dorsal (**J2**, **K2**), lateral (**A**–**D**, **H2**, **I2**), ventral (**L2**), and indet. (**N**–**Q**)

diagnostic characters, cannot be confidently identified beyond Anura indet.

General description, comparisons and remarks: Cranial elements include maxillary fragments up to 2.7 mm in length (AMU-CURS-723, -1149, -1162, and -1165–1166) preserving some dental positions, but not complete teeth (Fig. 14C1–F2). Postcranial elements include a distal fragment of a ?right ilium of 2.19 mm in length (AMU-CURS-1150, Fig. 14G), a distal portion of left humerus of 1.9 mm in length (AMU-CURS-1152, Fig. 14H), distal fragment of a right radioulna with a length of 4.2 mm (AMU-CURS-1151, Fig. 14J), and some fragmented vertebrae and other indeterminate limb bones (AMU-CURS-807 and -1153, Fig. 14I, K, L).

Testudines Batsch, 1788 [Joyce et al., 2020a].
Cryptodira Cope, 1868 [Joyce et al., 2020c]
Testudinidae Gray, 1825a, b [Joyce et al., 2021]
Chelonoidis Fitzinger, 1835
Chelonoidis sp.
(Fig. 15A1–A3).

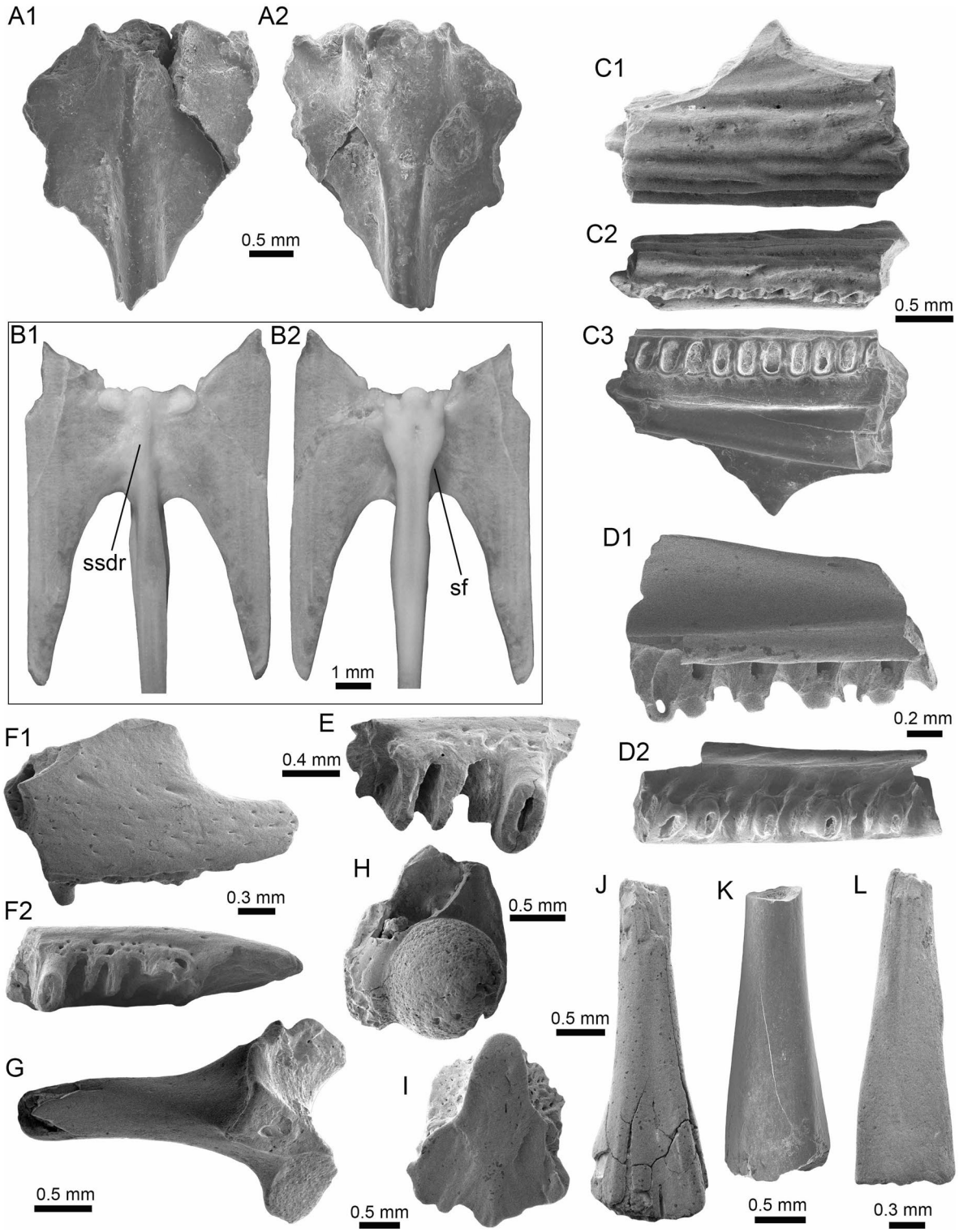

Fig. 14 Anura from the Vergel Member. **A1**, **A2** Incomplete fused sacral vertebra of cf. *Pipa* sp. (AMU-CURS-722). **B1**, **B2** Sacral vertebra of recent *Pipa parva* (PIMUZ A/II 118). **C1**–**L** Anura indet. **C1**–**F2** Maxilla fragments (**C1**–**C3** AMU-CURS-1177, **D1**, **D2** AMU-CURS-1149, **E** AMU-CURS-1166 and **F1**, **F2** AMU-CURS-1165). **G** Distal fragment of a left ilium (AMU-CURS-1150). **H** Distal portion of left humerus (AMU-CURS-1152). **I** Spinous process of and incomplete trunk vertebra (AMU-CURS-1153). **J** Distal fragment of a right radioulna (AMU-CURS-1151). **K**, **L** Indeterminate limb bone fragments (AMU-CURS-807). Views: dorsal (**A1**, **B1**, **I**, ?**J**), left lateral (**G**), right lateral (**F1**), lateral (**C1**, **D1**), lateroventral (**C2**), ventral (**A2**, **B2**, **C3**, **D2**, **E**, **F2**, **H**), and indet. (**K**, **L**). *ssdr* sacral sagittal dorsal ridge, *sf* spinal foramen

Locality: NCC (conglomerate, Fig. 3B).

Material: An incomplete right femur (AMU-CURS-584).

General description, comparisons and remarks: AMU-CURS-584 has a length of 70 mm, preserving the shaft, part of the proximal metaphysis and the distal epiphysis. Although the distal articular surface of the specimen is not perfectly preserved, the articular facets are clearly visible. Morphological features of specimen AMU-CURS-584 coincide with those observed in femora of extinct (e.g., Turvey et al. 2017) and extant *Chelonoidis* (e.g., *Chelonoidis carbonarius* and *Chelonoidis denticulatus*).

Pleurodira Cope, 1865 [Joyce et al., 2020b]
Chelidae Lindholm, 1929 [Joyce et al., 2021]
Chelus Duméril, 1806
Chelus sp.
(Fig. 15B1, B2).

Locality: NCC (conglomerate, Fig. 3B).

Material: The specimen corresponds to a plastron fragment (AMU-CURS-839).

General description, comparisons and remarks: AMU-CURS-839 is 36 mm in length. It constitutes the anterolateral portion of a left xiphiplastron, exhibiting on its ventral surface a densely vermiculated bone surface, and preserving the beginning of the thick xiphiplastron tip characteristics of *Chelus*. On the dorsal surface (Fig. 15B1), a portion of the pubis is preserved.

Podocnemididae Cope, 1868 [Joyce et al., 2021]
Podocnemididae indet.
(Fig. 15C1–L2).

Locality: NCC (conglomerate, Fig. 3B) and SGOP (conglomerate Ly1, Fig. 3C).

Material: A total of 51 postcranial remains: 48 from NCC (AMU-CURS-79, -547, -555, -560, -567, -571–572, -579–580, -675, -763, -838, and -866) and three from SGOP (AMU-CURS-1305–1307) localities.

General description, comparisons and remarks: The specimen AMU-CURS-571 constitutes a cervical vertebra (Fig. 15C1–C5), resembling in length, height, and morphology cervical 3 of the extant *Podocnemis expansa* (AMNH 62947). The prezygapophyses are projected dorsally with rounded tips. The postzygapophyses are laterally projected, exhibiting a facet for the articulation with cervical 4. The posterior condyle has a horse-saddle shape, which is the most typical condition of cervicals 3 to 7 in podocnemidids. The ventral portion of the centrum lacks a keel and forms a slightly concave margin. AMU-CURS-675 is a nearly complete left ilium, preserving part of the concave acetabulum (Fig. 15D), and AMU-CURS-1305 constitutes a nearly complete left ischium, missing some portions of its most ventrodistal edge (Fig. 15E1, E2). Dorsoproximally, the latter exhibits the sutural surface that articulates with the pubis and ilium, as well as a smooth surface that makes part of the acetabulum capsule. In all its aspects, AMU-CURS-1305 resembles the left ischium of extant and fossil podocnemidids, as in *Podocnemis expansa* (AMNH-62947).

Carapace and plastron fragments ($n = 48$) are the most abundant podocnemidids remains in the NCC locality. AMU-CURS-547 corresponds to a lateral portion of a costal bone (Fig. 15I1, I2), potentially left costal 5, considering that it has the inguinal scar and on the ventral surface it lacks evidence of a sulcus between pleural scutes. It is attributed to podocnemidids, based on smoothly sculpted dorsal bone surface, and thinner thickness of the same, in contrast to representatives of the *Chelus* genus that also occur in the Vergel Member. AMU-CURS-555 corresponds to a lateral portion of a potential right costal 5, exhibiting a portion of the inguinal scar on its ventral surface. The specimen AMU-CURS-560 represents the medial portion of a costal bone, potentially left costal 3, exhibiting a smooth dorsal bone surface and marks of the sulci between pleural and vertebral scutes. AMU-CURS-567 is the medial portion of a costal bone, potentially right costal 8. On the dorsal surface, the sulcus between vertebral and pleural scutes is clearly defined, and on the ventral surface a portion of the iliac scar is preserved. AMU-CURS-572A is a neural bone, missing its anterior portion. Its dorsal surface is eroded and there is no clear evidence of a sulcus. AMU-CURS-866 is a neural 1, missing its anterior portion. On its dorsal surface the sulcus between vertebral scutes is visible. On the ventral surface, the scar for the attachment of the thoracic vertebra is preserved. AMU-CURS-572B represents a complete peripheral bone from the posterior margin of the carapace. On its dorsal surface, the sulci between marginal and pleural scutes are visible and well defined. AMU-CURS-579 corresponds to an isolated peripheral bone from the carapace–plastron bridge region (Fig. 15L1, L2); on its dorsal surface, the sulcus between marginal scutes is visible. The medial edge (sutural contact with the costal) has been affected by bioerosion creating pits between the serrated bone textures. AMU-CURS-1306 is a costal bone (Fig. 15J), potentially the right costal 6, due to the relatively straight medial margin and the sulci between vertebral and pleural scutes on its dorsal surface. In ventral view, the costal rib process is well defined. AMU-CURS-1307 corresponds to a peripheral bone from the posterior margin of the carapace (Fig. 15F). In dorsal view, the sulci between marginal and pleural scutes are well defined, as well as some

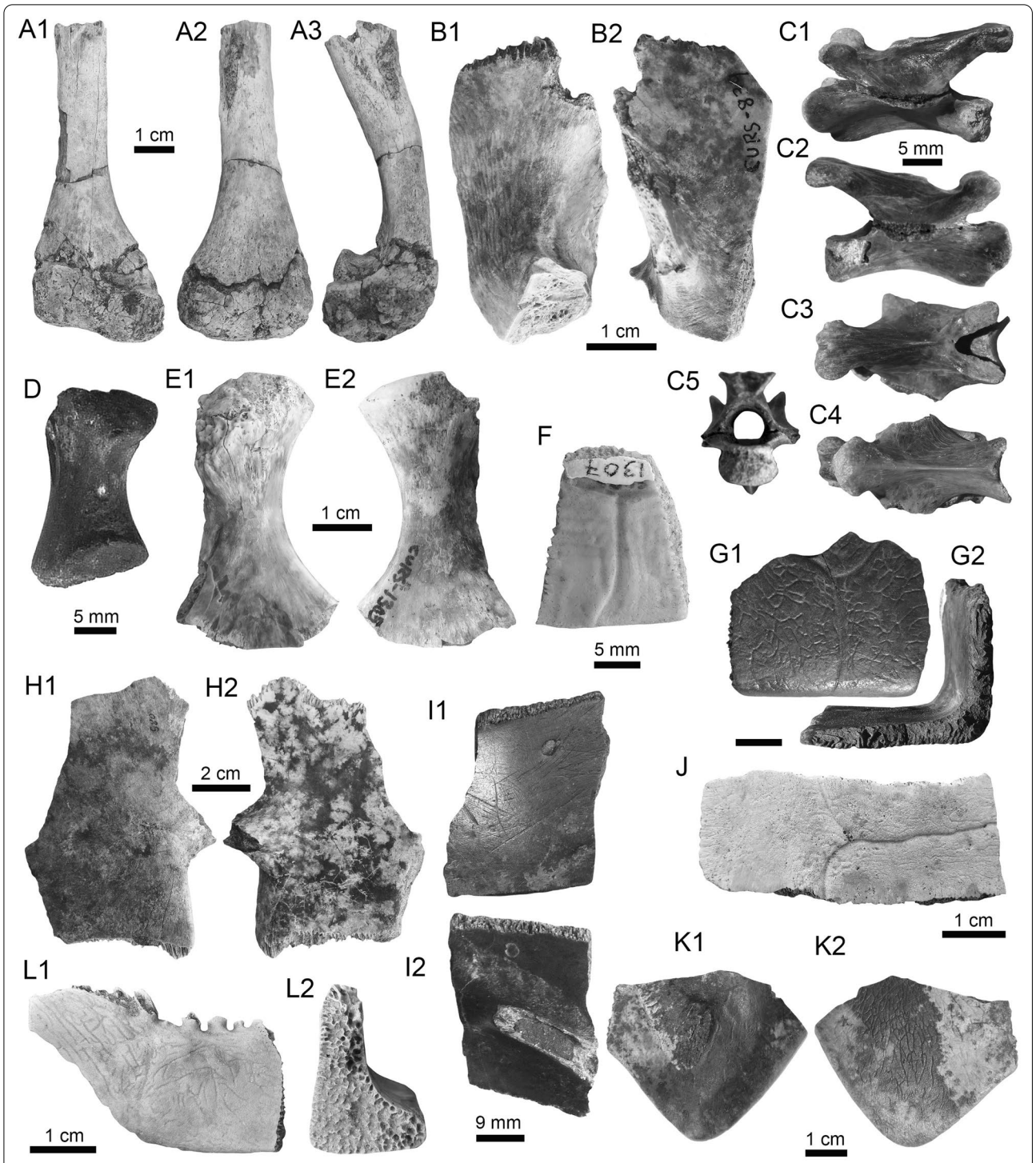

Fig. 15 Testudines (Testudinidae, Chelidae, and Podocnemididae) from the Vergel (**A1**–**D**, **G1**–**I2**, **K1**–**L2**) and Cocuiza (**E1**–**F**, **J**) members. **A1**–**A3** Incomplete right femur of *Chelonoidis* sp. (AMU-CURS-584). **B1**, **B2** Anterolateral portion of a left xiphiplastron of *Chelus* sp. (AMU-CURS-839). **C1**–**K2** Podocnemididae indet. **C1**–**C5** Cervical vertebra (AMU-CURS-571). **D** Left ilium (AMU-CURS-675). **E1**, **E2** Left ischium (AMU-CURS-1305). **F** Peripheral bone from the posterior margin of the carapace (AMU-CURS-1307). **G** Peripheral bone from the bridge region of the shell (AMU-CURS-838). **H1**, **H2** Partial right hypoplastron (AMU-CURS-580). **I1**, **I2** Lateral portion of a costal bone, potentially left costal 5 (AMU-CURS-547). **J** Costal bone potentially the right costal 6 (AMU-CURS-1306). **K1**, **K2** Posterior tip of a right xiphiplastron (AMU-CURS-79). **L1**, **L2** Peripheral bone from the carapace-plastron bridge region (AMU-CURS-579). Views: anterior (**A2**), dorsal (**C3**, **E1**, **F**), cross-sectional (**G2**, **L2**), internal (**B1**, **H2**, **I2**, **K1**), external (**B2**, **H1**, **I1**, **J**, **K2**, **L1**), left lateral (**C1**), right lateral (**A3**, **C2**), lateral (**D**, **G1**), posterior (**A1**, **C5**), and ventral (**C4**, **E2**)

annuli lines close to the boundary between marginal and the pleural.

AMU-CURS-838 corresponds to a nearly complete peripheral bone from the bridge region of the shell (Fig. 15G1, G2). On its dorsal surface, the sulci between marginals and pleural scutes are visible, as well as a dichotomic sculpturing bone surface, which can be the case of shells of some extant podocnemidids, for example, *Podocnemis lewyana*. AMU-CURS-79 represents the posterior tip of a right xiphiplastron (Fig. 15K1, K2); the dorsal surface of the ischial scar is preserved, indicating that both ischia met medially. The specimen AMU-CURS-580 is a partial right hypoplastron (Fig. 15H1, H2), missing part of its lateral region and most of the anteromedial region. On its ventral surface, the abdominofemoral sulcus is visible. Due to the absence of diagnostic characteristics defining possible morphotypes in the sample, we can only justify the presence of at least one podocnemidid taxon.

Testudines indet.
(Fig. 16A–E).

Locality: NCC (conglomerate, Fig. 3B).

Material: An assortment of 85 fragmentary and poorly preserved cranial and some postcranial bones and carapace/plastron remains (AMU-CURS-561, -569, -581, -693, -735, -840–844, -862, -883, -1059, -1122, -1154, -1160, -1185, and -1288–1289).

General description, comparisons and remarks: Due to their preservation, these remains lack diagnostic elements that allow a more confident assignment (e.g., Fig. 16D–E). Among the most representative elements that can be referred are a fragment of a small right premaxilla of 11.7 mm in length (AMU-CURS-1154, Fig. 16A), the distal section of a left fibula of 21 mm in length (AMU-CURS-1160, Fig. 16B1, B2), and a plastron fragment with a clear round bite mark (AMU-CURS-862, Fig. 16C1, C2).

Squamata Oppel, 1811b
Teiidae Gray, 1827
Tupinambis Daudin, 1802
Tupinambis s.l.
(Fig. 16F1–F3).

Locality: NCC (conglomerate, Fig. 3B).

Material: A fragmentary right dentary (AMU-CURS-721).

General description, comparisons and remarks: AMU-CURS-721 is 37 mm long and posteriorly and posteroventrally incomplete. In medial view (Fig. 16F3), the Meckel's canal is entirely open (it reaches the posterior edge of the dentary symphysis) and broad. No teeth are preserved but they were clearly subpleurodont and surrounded by a porous tissue. A thick subdental shelf (3.7 mm) preserves the first 11 tooth positions, plus the anterior wall of the 12th position. The dental shelf is of uniform height up to the ninth tooth position, but thins slightly posteriorly. The remnants of the teeth indicate that their base was approximately cylindrical (but the last preserved tooth was slightly compressed labiolingually) and that their size decreased posteriorly up the fifth position and then increased up to the last preserved tooth that was clearly the largest of the preserved series (Fig. 16F1). Despite the presence of a matrix filling the concavities, it seems that medial to each tooth position there is a replacement socket, longer than it is wide. Along the posterior section of the dentary, a small tooth cusp is visible among the matrix filling the replacement socked of the 11th tooth position. The dentary symphysis reaches the level of the fifth alveolus. The outer surface of the dentary (Fig. 16F2) hosts six dental foramina aligned parallel to the straight dorsal edge of the element, and closer to it than to the ventral edge. Irregular postmortem traces are present on the outer surface.

The general morphology of AMU-CURS-721 matches that of large-sized teiid (Estes 1983; Nydam et al. 2007). It differs from that of *Dracaena* because of the higher number of tooth positions present in the symphysis and the higher number of small anterior teeth (actually tooth positions in AMU-CURS-721; Estes 1961). AMU-CURS-721 differs from extinct †*Paradracaena colombiana* (Estes 1961) (originally described from the middle Miocene of Colombia, Estes 1961, but also present in the Miocene of Brazil, Hsiou et al. 2009, and Peru, Pujos et al. 2009) in the nearly straight orientation of the dorsal edge of the dentary. Conversely, the morphology of AMU-CURS-721 is broadly congruent with that of *Salvator* and *Tupinambis*, whose comparative osteological diagnosis is still unknown (Hsiou et al. 2016) despite it having a relevant interest for paleontologists due to the rich fossil record of *Tupinambis*-like taxa (see Albino et al. 2006; Albino and Brizuela 2014). Waiting for a full description of the dentary of these two recently separated taxa (Harvey et al. 2012), AMU-CURS-721 is here referred to *Tupinambis* s.l. It is worth mentioning that *Tupinambis* is the only large-sized teiid currently inhabiting Falcón State (Mijares-Urrutia and Arends 2000).

(non-snake) Squamata indet.
(Fig. 16G–K).

Locality: NCC (conglomerate, Fig. 3B).

Material: Five cranial elements in a fragmentary condition (AMU-CURS-725, -797, -1148, and -1163–64).